



HAL
open science

Anatexis of accretionary wedge, Pacific-type magmatism, and formation of vertically stratified continental crust in the Altai Orogenic Belt

Yuchao Jiang, K. Schulmann, M. Sun, P. Štípská, A. Guy, V. Janoušek, O. Lexa, C. Yuan

► To cite this version:

Yuchao Jiang, K. Schulmann, M. Sun, P. Štípská, A. Guy, et al.. Anatexis of accretionary wedge, Pacific-type magmatism, and formation of vertically stratified continental crust in the Altai Orogenic Belt. *Tectonics*, 2016, 35 (12), pp.3095 - 3118. 10.1002/2016TC004271 . hal-01615633

HAL Id: hal-01615633

<https://hal.science/hal-01615633v1>

Submitted on 22 Oct 2021

HAL is a multi-disciplinary open access archive for the deposit and dissemination of scientific research documents, whether they are published or not. The documents may come from teaching and research institutions in France or abroad, or from public or private research centers.

L'archive ouverte pluridisciplinaire **HAL**, est destinée au dépôt et à la diffusion de documents scientifiques de niveau recherche, publiés ou non, émanant des établissements d'enseignement et de recherche français ou étrangers, des laboratoires publics ou privés.

Copyright

RESEARCH ARTICLE

10.1002/2016TC004271

Key Points:

- Ordovician accretionary wedge sediments in the Chinese Altai may be a viable source for Pacific-type Silurian-Devonian granitoids
- Melting of accretionary wedge left behind granulitic residue that can explain gravity high over the Chinese Altai
- Melting and crustal differentiation of the accretionary wedge sediments can transform oceanic material into stabilized continent

Supporting Information:

- Supporting Information S1
- Table S1
- Table S2
- Table S3
- Table S4
- Table S5

Correspondence to:

Y. D. Jiang,
jiangyd@gig.ac.cn

Citation:

Jiang, Y. D., K. Schulmann, M. Sun, P. Štípská, A. Guy, V. Janoušek, O. Lexa, and C. Yuan (2016), Anatexis of accretionary wedge, Pacific-type magmatism, and formation of vertically stratified continental crust in the Altai Orogenic Belt, *Tectonics*, 35, 3095–3118, doi:10.1002/2016TC004271.







Received 8 JUN 2016

Accepted 5 DEC 2016

Accepted article online 9 DEC 2016

Published online 27 DEC 2016

Anatexis of accretionary wedge, Pacific-type magmatism, and formation of vertically stratified continental crust in the Altai Orogenic Belt

Y. D. Jiang^{1,2,3} , K. Schulmann^{2,4}, M. Sun⁵, P. Štípská^{2,4} , A. Guy² , V. Janoušek² , O. Lexa³ , and C. Yuan¹ 

¹State Key Laboratory of Isotope Geochemistry, Guangzhou Institute of Geochemistry, Chinese Academy of Sciences, Guangzhou, China, ²Center for Lithospheric Research, Czech Geological Survey, Prague, Czech Republic, ³Institute of Petrology and Structural Geology, Charles University, Prague, Czech Republic, ⁴EOST, Institut de Physique du Globe, UMR 7516, Université de Strasbourg, Strasbourg, France, ⁵Department of Earth Sciences, University of Hong Kong, Hong Kong

Abstract Granitoid magmatism and its role in differentiation and stabilization of the Paleozoic accretionary wedge in the Chinese Altai are evaluated in this study. Voluminous Silurian-Devonian granitoids intruded a greywacke-dominated Ordovician sedimentary succession (the Habahe Group) of the accretionary wedge. The close temporal and spatial relationship between the regional anatexis and the formation of granitoids, as well as their geochemical similarities including rather unevolved Nd isotopic signatures and the strong enrichment of large-ion lithophile elements relative to many of the high field strength elements, may indicate that the granitoids are product of partial melting of the accretionary wedge rocks. Whole-rock geochemistry and pseudosection modeling show that regional anatexis of fertile sediments could have produced a large amount of melts compositionally similar to the granitoids. Such process could have left a high-density garnet- and/or garnet-pyroxene granulite residue in the deep crust, which can be the major reason for the gravity high over the Chinese Altai. Our results show that melting and crustal differentiation can transform accretionary wedge sediments into vertically stratified and stable continental crust. This may be a key mechanism contributing to the peripheral continental growth worldwide.

1. Introduction

Average continental crust has subduction-related trace element signatures. It is therefore widely accepted that continental crust is dominantly generated at convergent margins via arc magmatism [Taylor, 1967; Rudnick, 1995; Jagoutz and Schmidt, 2012]. However, the primitive arc magma is predominantly of basaltic bulk composition unlike the broadly andesitic continental crust, and this has become a problem known as the “continental crust composition paradox” [Rollinson, 2008]. As a solution it has been suggested that primitive basaltic melts or a possibly initially more basaltic bulk arc crust can be differentiated toward an evolved continental crust through either fractional crystallization or remelting followed by the removal of ultramafic cumulates from the lower crust back into the mantle [e.g., Anderson, 1982; Rudnick, 1995; Holbrook et al., 1999]. The differentiation can eventually result in the formation of mature continental crust characterized by a granitic upper portion and a residual, mafic lower portion [Ringwood, 1974; Solano et al., 2012]. The occurrence of granitic rocks in arcs is therefore accepted as the most conspicuous feature indicating the establishment of a mature continental crust [e.g., Baker, 1968; Rudnick and Gao, 2003].

Pacific-type convergent margins are characterized by giant accretionary wedges formed by scraping off oceanic sediments from the subducting plate [Cawood et al., 2009]. It has been proposed that anatexis of these fertile sediments could produce voluminous granitic magmas and stabilize the accretionary wedge [Brown, 2010; Yakymchuk et al., 2013], but no details regarding the exact mechanism of crustal differentiation and formation of mature continental crust were given. This gap can be filled by the study of magmatic evolution of the Altai Orogenic Belt, which represents a high-grade core of the Central Asian Orogenic Belt (CAOB), the latter considered to be the Earth’s largest area of Phanerozoic crustal growth [Şengör et al., 1993; Windley et al., 2007].

The Altai Orogenic Belt is mainly composed of variably metamorphosed Ordovician sedimentary sequence and voluminous Silurian-Devonian granitoids (about 40% of the map surface) [Zou et al., 1988]. Geophysical surveys have shown that this region is characterized by high seismic *P* wave velocities (6.9–7.0 km/s) of the

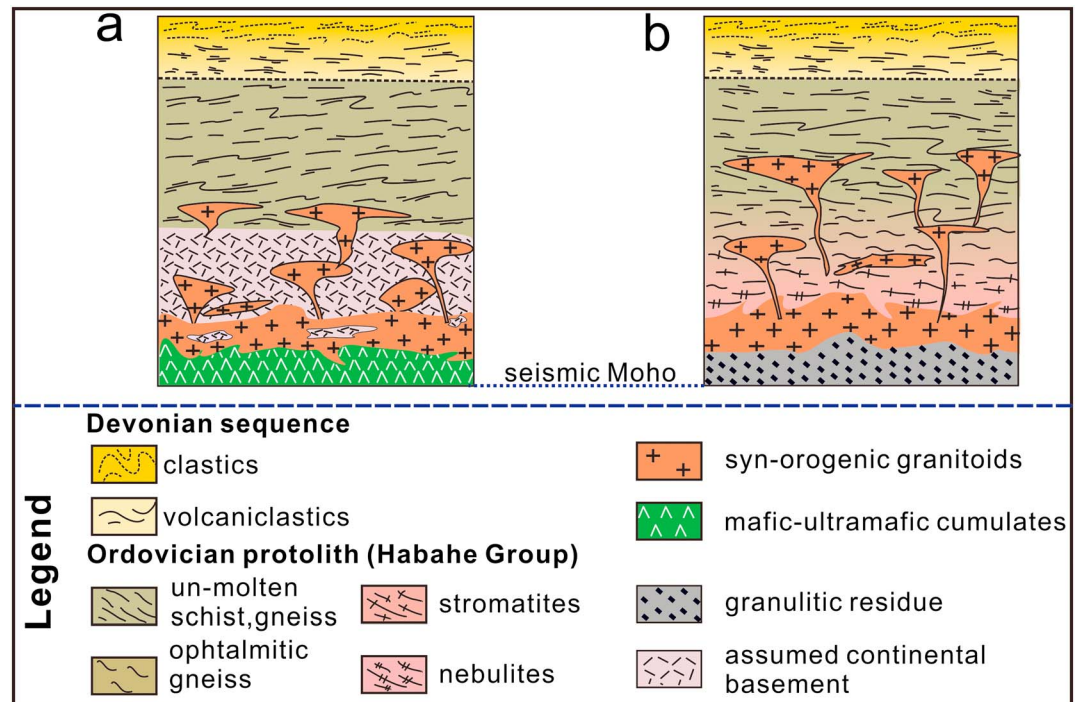


Figure 1. Competing views on the orogenic crustal architectures of the Chinese Altai based (a) on geochemical studies [e.g., Wang et al., 2009] and (b) on structural and petrological studies [e.g., Jiang et al., 2015].

lower crust consistent with the presence of either mafic granulite or metaperidotite with some granulitic metapelite and by middle and upper crustal layers (P wave velocities 6.6 and 6.1 km/s) indicative of an intermediate and a quartz-rich granitic crustal compositions, respectively [Wang et al., 2003]. These characteristics indicate that the deep structure of the Altai Orogenic Belt shows a three-layer stratification of the crust typical of stable continents, perhaps a result of partial melting and crustal differentiation after Paleozoic terrane accretion.

The apparently subduction-related geochemical characteristics of the Chinese Altai granitoids were classically interpreted as a product of arc magmatism established on an old Precambrian basement and its Paleozoic sedimentary cover [Wang et al., 2006]. Their relatively primitive Sr-Nd isotopic signatures have led to the interpretation that they were generated by massive influx of depleted mantle-derived components [Jahn et al., 2000, 2004; Wang et al., 2009]. This resulted in a tectonic model of large-scale basaltic magma underplating beneath an old continental crust and intrusion of mixed mantle and crustal magmas into middle and upper crustal metasedimentary cover (Figure 1a). However, such a model is at odds with the recent geochronological studies, which have proven that the previously thought Precambrian continental basement, i.e., high-grade metamorphic rocks, is, in fact, Ordovician [e.g., Sun et al., 2008]. The presence of Precambrian continental basement and hence the whole petrogenetic model of magmatic reworking of an old continental crust are therefore highly speculative. Consequently, the Chinese Altai rocks were reinterpreted as variably metamorphosed accretionary wedge consisting of Ordovician sedimentary sequence without any continental basement [Long et al., 2008; Xiao et al., 2009; Jiang et al., 2011]. In addition, structural, metamorphic petrology, and geochronology studies indicate that anatexis of Ordovician metasediments was coeval with the main Devonian magmatic pulse [Jiang et al., 2010, 2015]. Based on these findings, we discuss a possibility that this giant accretionary complex was partially molten at deep crustal levels, producing Devonian granitoids intruding low- to medium-grade sedimentary rocks in the upper crust and leaving behind a lower crustal granulitic residue (Figure 1b).

We focus on the magmatic evolution of the Chinese Altai aiming to address the issues of (1) the sources of granitoid magmatism and (2) the role of crustal melting in formation of vertically stratified crust in accretionary orogens. The first question is answered by reevaluation of geochemical and petrological data of the Altai Silurian-Devonian granitoids and by thermodynamic modeling of various aspects of melting the

greywacke-dominated Ordovician sedimentary sequence. This approach shows that young accreted metasediments can also be a source of the “arc-like” granitoid magmatism. Subsequently, the densities of both molten and unmolten accreted Ordovician metasediments are thermodynamically modeled and interpreted in the frame of gravity and seismic data from the Altai Mountains. Finally, we discuss the two petrogenetic models of the Altai granitoids as well as results of gravity modeling in light of geological observations from critical Chinese Altai crustal sections. The Altai crustal architecture and isotopic signature of its granitoids are compared with European Variscan (Pyrenees) section that represents a type region of basaltic underplating of continental basement. Based on this comparison, we propose a model of crustal differentiation and formation of mature continental crust in accretionary orogens.

2. Geological Framework of the Chinese Altai

The CAOB consists of magmatic arcs, ophiolites, accretionary wedges, passive margins, and microcontinents, which have been assembled from Neoproterozoic to Late Paleozoic [Şengör *et al.*, 1993; Wilhem *et al.*, 2012]. Şengör *et al.* [1993] proposed that the entire Paleozoic domain of central Asia evolved from one single giant island arc (the Kipchak-Tuva-Mongol arc) and that most Paleozoic magmatic rocks were primitive in origin, implying that nearly half of the CAOB crust is juvenile as well. Such a Pacific-type subduction model was advocated also by Jahn *et al.* [2004] who, based on Sr-Nd isotopic data of numerous granitoids, considered the CAOB crust to be formed mainly by net crustal growth mechanism. On the other hand, several authors proposed an alternative subduction-collision mechanism involving multiple subduction of linear elements, microcontinent amalgamation, and oroclinal bending [Windley *et al.*, 2007; Xiao *et al.*, 2009; Lehmann *et al.*, 2010] with strong component of magmatic recycling [Kovalenko *et al.*, 2004; Kovach *et al.*, 2011; Kröner *et al.*, 2014].

The SW Mongolian and NW Chinese tracts of the CAOB comprise the following tectonostratigraphic units from NE to SW (Figure 2): the Precambrian Tuva-Mongolian ribbon continent, a Neoproterozoic ophiolitic belt intruded by Early Cambrian arc magmas [Soejono *et al.*, 2016]—the Lake Zone, a giant and variably metamorphosed Early Paleozoic sedimentary succession intruded by Silurian-Devonian granitoids forming the Hovd-Altai Zone (Figure 2) [Kröner *et al.*, 2010]. In the south unmetamorphosed Devonian and Carboniferous ocean floor sequences called the Trans-Altai Zone in Mongolia and the Junggar Terrane in China occur. The detailed lithostratigraphic, geochronological, and structural features of these units were summarized by Badarch *et al.* [2002], Windley *et al.* [2002], and Wilhem *et al.* [2012].

The Altai Orogenic Belt (including the Chinese and the Mongolian Altai) is characterized by low- to medium-grade Ordovician and Devonian sedimentary sequences alternating with NW-SE trending elongated domes cored by migmatites and granitoids. These rocks are separated in the south from unmetamorphosed Paleozoic ocean floor sediments and volcanic rocks of the eastern Junggar Terrane (Chinese equivalent of the Trans-Altai Zone) by the Erqis Fault [Xiao *et al.*, 2009]. The Chinese segment of the Altai Orogen, namely, the Chinese Altai, represents an important high-grade core of the whole Hovd-Altai Zone. In the following text, we mainly summarize available petrological, geochronological, and geochemical aspects on the Ordovician sedimentary sequences and Silurian-Devonian granitoids of the Chinese Altai.

2.1. Ordovician Metasedimentary Sequence of the Habahe Group

The Habahe Group is the oldest and most extensive lithological unit in the studied region, and it extends for ~2500 km from the Chinese and Mongolian Altai in the southeast to Russian and Kazakh Altai in the northwest. It consists of dominant terrigenous-clastic and subordinate volcanoclastic rocks, tuffaceous sediments, and volcanic rocks [Windley *et al.*, 2002; Xiao *et al.*, 2009]. The geochemistry of terrigenous sedimentary components suggests that they are chemically immature and compositionally similar to greywacke (Figure 3a) and could be interpreted as detritus deposited in an active margin setting with significant volcanic input (Figure 3b) [see also Long *et al.*, 2008]. This is further supported by the trace element characteristics of these terrigenous sediments, which have patterns resembling immature Pacific trench sediments but showing lower concentrations of large-ion lithophile element (LILE) (e.g., Rb, Sr, Ba, Th, U, and Pb) and high field strength element (HFSE) (e.g., Zr, Hf, Nb, and Ta) than the mature post-Archean Australian shale (PAAS; see Figure 3c). Such tectonic environment is also manifested by the La/Sc versus Ti/Zr tectonic discrimination diagrams of Bhatia and Crook [1986], which indicates that the sediments of the Habahe Group were deposited in continental arc/active continental margin settings (Figure 3d).

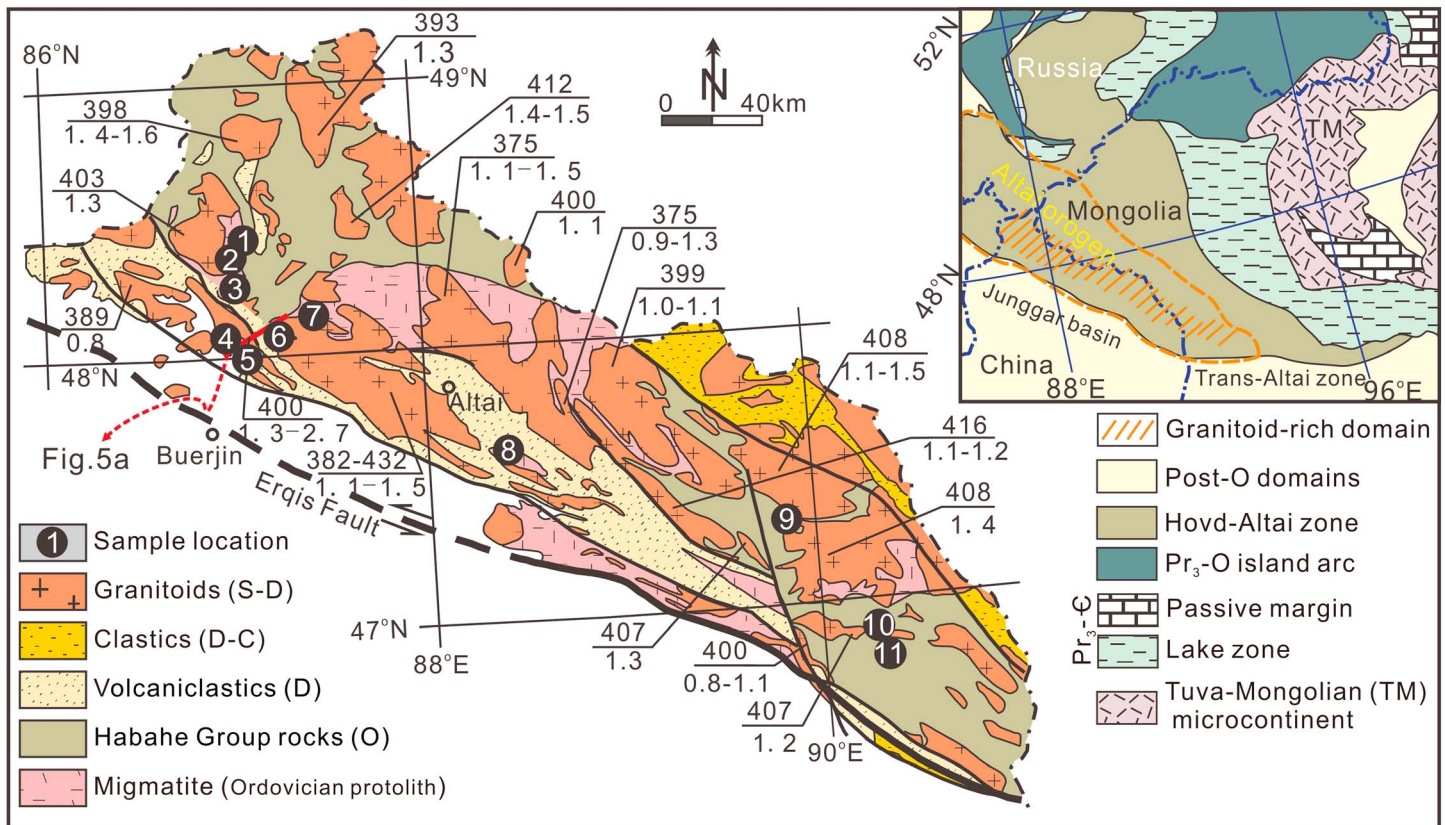


Figure 2. Geological map of the NW Chinese and western Mongolian tract of the CAOB (upper right) and the geological map of the Chinese Altai (lower left), showing localities of samples collected for Nd isotopic analysis in this study. Emplacement ages (Ma) and Nd model ages (Ga) for granitoids from literature [Wang et al., 2009; Cai et al., 2012] are also indicated.

Recent studies suggested that the detrital zircon age patterns of the Habahe Group can be explained by the contribution of arc-related rocks in the Lake Zone and Precambrian basement of the Tuva-Mongolian block to the sedimentary basin [e.g., Jiang et al., 2011], consistent with the notion of fairly significant input of volcanic components to the sedimentary basin. In addition, it has been documented that more than 70% of the detrital zircons from the Habahe Group have positive zircon $\epsilon_{\text{Hf}}(t)$ values, suggesting that the metasediments contained an abundant young and geochemically primitive component [Cai et al., 2011a]. An Early Paleozoic Barrovian-type metamorphic zonation is developed in the Habahe Group as well as in its southern Mongolian equivalent (Tugrug Formation), indicating maximum burial to depth of >30 km (Figure 4) [see also Wei et al., 2007; Broussolle et al., 2015; Jiang et al., 2015]. Based on available petrographic data (Figure 4), it is suggested that the deeply buried Habahe Group experienced subsequent high-temperature reequilibration under high geothermal gradient (~30°C/km). The ensuing deep crustal anatexis at 700–1000°C (Figure 4) [see also Wei et al., 2007; Li et al., 2014; Jiang et al., 2015] has been dated as Middle Devonian (zircon U-Pb ages of 390–380 Ma) [Kozakov et al., 2002; Jiang et al., 2010]. Then vertical extrusion of partially molten lower crustal rocks resulted in elongated large migmatite-magmatite domes alternating with metasedimentary synforms (Figure 5a) [see also Jiang et al., 2015].

2.2. Granitoids and Their Eruptive Equivalents

Abundant granitoids intruded the Ordovician Habahe sequence mainly in the southern Altai (Figure 2). They form isolated circular or elongate bodies, locally associated with subordinate gabbroic intrusions. Many granitoids were syntectonic, coeval with the formation of the migmatite-magmatite domes (Figure 5a, modified after Jiang et al. [2015]). These intrusions are surrounded by high-grade gneisses which developed pervasive subvertical S2 foliation defined by the preferred orientation of sillimanite and biotite (Figure 5b). Toward the granitoids, the gneisses show progressive textural evolution of migmatite types, from ophthalmic gneisses,

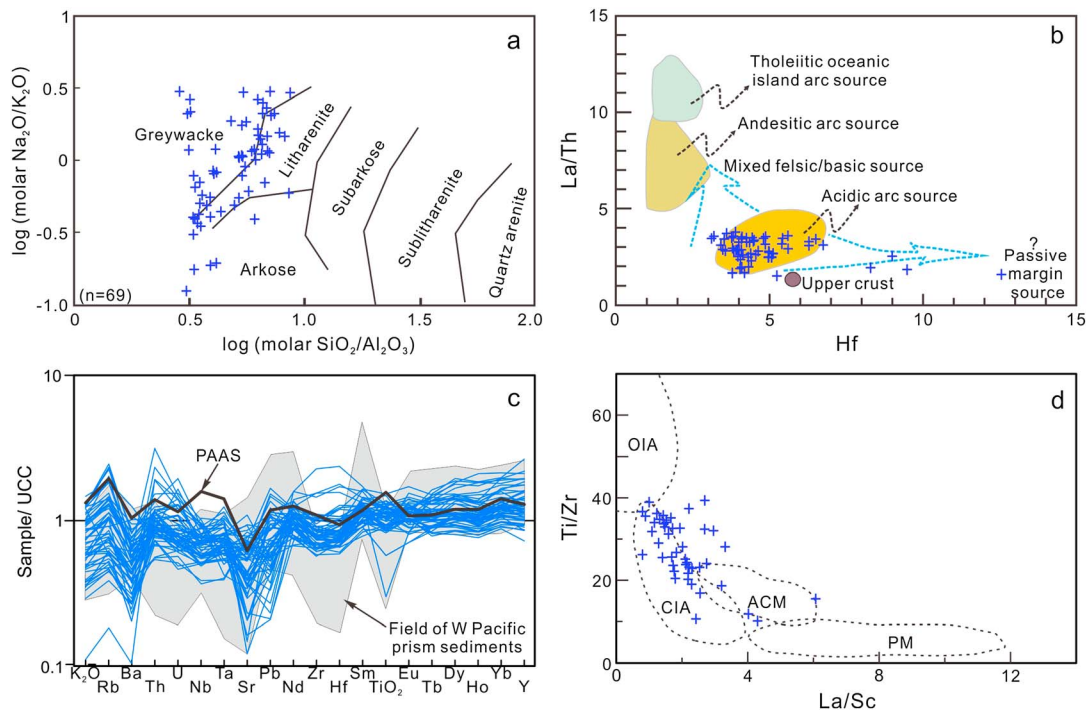


Figure 3. Geochemical characteristics of the Ordovician Habahe Group terrigenous sedimentary rocks from the Chinese Altai. (a) Classification diagram after *Pettijohn et al.* [1987], showing their greywacke-dominated nature. (b) Hf versus La/Th diagram after *Floyd and Leveridge* [1987], suggesting significant input of acidic arc sources. (c) Upper continental crust (UCC) normalized trace element patterns for the Habahe Group terrigenous sediments. The normalizing values are from *Taylor and McLennan* [1985]. Literature chemical data from Pacific-type trench sediments of *Plank and Langmuir* [1998] and Post-Archean Average Shale (PAAS) of *Taylor and McLennan* [1985] are shown for comparisons. (d) La/Sc versus Ti/Zr diagram [after *Bhatia and Crook*, 1986], suggesting a continental arc/active continental margin setting. Outlined fields: OIA= oceanic island arc; CIA= continental arc; ACM= active continental margin; and PM= passive margin. Details on data sources are available in the supporting information S1 and presented in Table S1.

through stromatolites to nebulites (Figure 5) and are associated with garnet- and/or muscovite-bearing leucogranite bodies (Figure 5b). Rare kyanite relics are locally present in the migmatite (Figure 5b), evidencing deep burial of the protolith before the main generally sillimanite-grade anatexis reworking [*Jiang et al.*, 2015]. Granitoids in the central parts of the domes generally show a strong linear fabric (L2) defined by subvertically oriented amphibole and biotite (Figure 5b). Most granitoids have emplacement zircon U-Pb ages ranging from 440 to 370 Ma with a peak at around 400–390 Ma (Figure 5b) [*Cai et al.*, 2011a], coeval with the high-temperature anatexis in the region (Figure 5b) [*Jiang et al.*, 2010]. Inherited zircons in many granitoids are dominantly Early Paleozoic in age (540–440 Ma) [*Sun et al.*, 2008; *Cai et al.*, 2011b], supporting a widespread Neoproterozoic-Ordovician source component. Such zircon inheritance patterns, particularly the high proportion of ~500 Ma zircons, are in accord with the most common age of the detrital zircons from the Ordovician Habahe Group metasediments [*Sun et al.*, 2008; *Cai et al.*, 2011b] and provide a strong evidence that precludes production of the granitoids from a Proterozoic basement.

Granitoids are mainly granodiorites to granites with calc-alkaline, predominantly peraluminous compositions (Figures 6a and 6b). They display light rare earth element (LREE)-rich chondrite-normalized REE patterns, with relatively flat heavy REE segments and moderate to strong negative Eu anomalies (Figure 6c). Such REE patterns are very similar to those of the Habahe Group metasediments, even though the granitoids have commonly higher REE abundances than the metasediments (Figure 6c). Most granitoids are enriched in LILE and depleted in HFSE (especially Ta, Nb, and Ti) in N-MORB (mid-ocean ridge basalt) normalized spidergrams, closely mimicking the patterns of the Habahe Group metasediments (Figure 6d) [see also *Wang et al.*, 2006; *Yuan et al.*, 2007; *Cai et al.*, 2011b].

Most granitoids (~85%) are biotite granodiorites to granites, which are compositionally comparable to partial melts derived from immature sediments dominated by metagreywacke, with only limited contribution from mature pelitic source [*Liu et al.*, 2012] (Figure 6e). Besides, a few granitoids (<15%) are hornblende bearing,

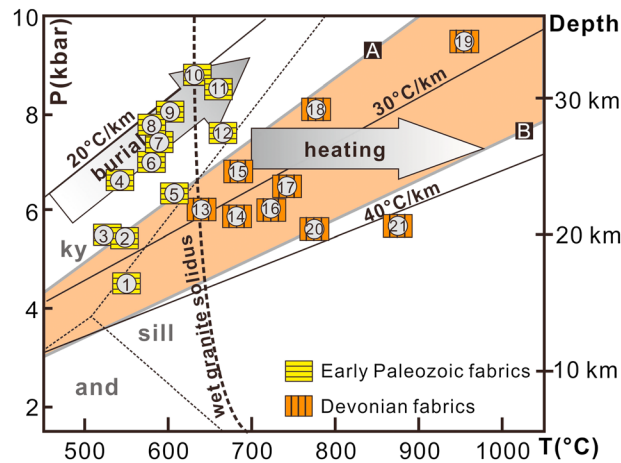


Figure 4. Geothermal gradients and published *P-T* estimates for peak metamorphic assemblages (Early-Middle Paleozoic ages) of the Habahe Group rocks and their southern Mongolian Altai equivalents (the Tugrug Formation). Wet granite solidus is after *Ebadi and Johannes* [1991]. Brown field highlights thermal conditions in Cascadia back-arc area of the central Andean extensional suprasubduction zone, which is limited by two geotherms for region with proposed surface heat flows of 80mW/m² (“A”) and 100mW/m² (“B”) [*Currie et al.*, 2004], respectively. These geotherms were calculated on the basis of respective mantle heat flow of 50 and 70mW/m² with conductivity of 2.25W/mK, thickness of radiogenic crust of 15km and radiogenic heat production of 2mW/m³, following the calculations and tectonic models of *Thompson et al.* [2001]. Data sources are available in the supporting information S1 and presented in Table S2.

calcic, and subaluminous (Figure 6b) [see also *Liu et al.*, 2012], comparable to partial melts derived from metatonalites (Figure 6f). Two thirds of granitoids have CaO/Na₂O ratios higher than 0.3 and typical are also relatively low Rb/Sr and Rb/Ba ratios (Figure 6f). They are thus chemically comparable with partial melts predominantly derived from clay-poor and plagioclase-rich sources, such as metagreywackes (Figure 6f). Only a few analyses resemble the compositions of pelite-derived melts and Himalayan peraluminous granite of *Sylvester* [1998].

3. Isotopic Analysis and Thermodynamic Modeling of Melting of the Habahe Group Rocks

In the current work, we use geochemical and thermodynamic modeling to assess the potential of the Ordovician greywacke-dominated Habahe Group rocks to be a source for the Silurian-Devonian arc-like granitoid magmatism. We first focus on Nd isotopic signatures (our own and published data; see supporting

information Table S3) from both the Habahe Group metasediments and the granitoids. Subsequently, compositions of the modeled melts are compared with those of the granitoids.

3.1. Nd Isotopic Signature of the Habahe Group Rocks and Devonian Granitoids

The $\epsilon_{Nd}(400\text{Ma})$ values of 12 Habahe terrigenous samples from this study and 19 previously published vary from -6.1 to +2.6 (mostly negative, Table S3), a range overlapping with, or somewhat less radiogenic than, most local granitoids and felsic volcanic rocks. The two-stage depleted mantle Nd model ages are 0.8–1.9 Ga (mostly 1.3–1.5 Ga, Table S3), again overlapping with those values for many granitoids and felsic volcanic rocks (0.6–1.5 Ga) [*Wang et al.*, 2009]. Such features support the view that the Habahe Group metasediments could be potentially the source of the granitoids.

It is traditionally considered that granitoids in the Chinese Altai originated by magma mixing of depleted mantle-derived and old crustally derived melts [e.g., *Wang et al.*, 2009]. Regardless of the exact mixing mechanism (magma mixing versus mixing of two components in the source), the proportion of the depleted mantle component can be evaluated using the binary mixing equation as follows:

$$\epsilon_m = [f_{DM} \times C_{DM} \times \epsilon_{DM} + (1-f_{DM}) \times C_{CC} \times \epsilon_{CC}] / [f_{DM} \times C_{DM} + (1-f_{DM}) \times C_{CC}]$$

where ϵ_m , ϵ_{DM} , and ϵ_{CC} refer to the epsilon Nd values of modeled magma, depleted mantle, and old continental crust, C_{DM} and C_{CC} to Nd concentrations in the depleted mantle-derived melt and the continental crust, and f_{DM} to the mass fraction of the depleted mantle in the magma source.

In previous works, a MORB-like basalt ($\epsilon_{Nd}(400\text{Ma})=+8$ and Nd=15 ppm [*Xu et al.*, 2003]) from the southeast Chinese Altai was taken as the equivalent of the depleted mantle-derived end-member and a paragneiss ($\epsilon_{Nd}(400\text{Ma})=-17$, Nd=36 ppm, depleted mantle Nd model age of 2.6 Ga [*Hu et al.*, 2000]) as the old continental end-member (hyperbola A-B in Figure 7a). In order to obtain the observed granitoid Nd isotopic characteristics (initial ϵ_{Nd} mostly ranging from -5 to +1), the required involvement of primitive basic components ranges mostly from 70% to 90% (Figure 7a) [see also *Jahn et al.*, 2004; *Wang et al.*, 2009]. However, MORB-like basalts often have lower Nd abundances. Thus, the shape of the mixing curve with the basalt poorest in Nd

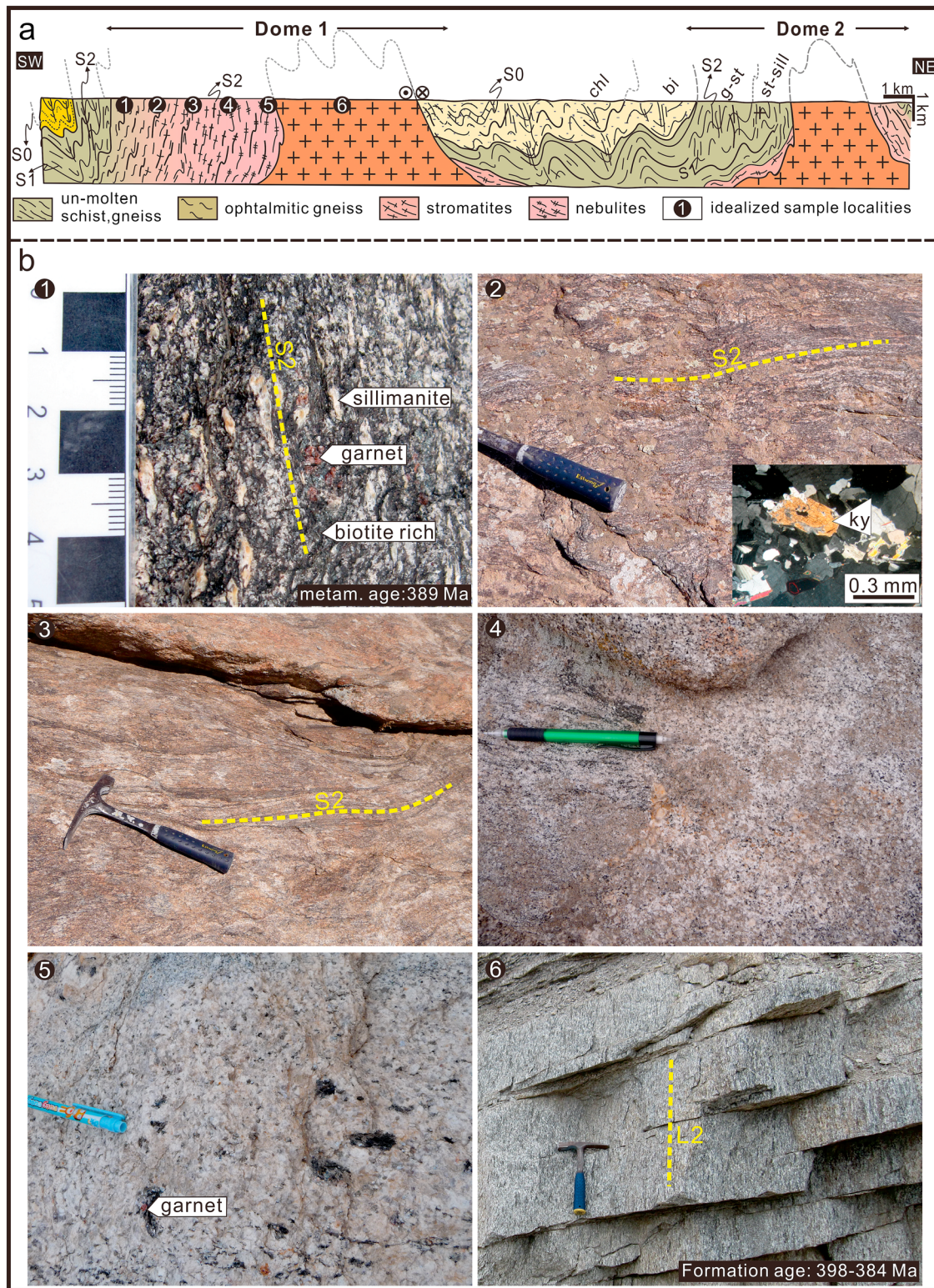


Figure 5. (a) Schematic cross section showing migmatite-magmatite domes in the Chinese Altai, including metamorphic isograds and structural relationships between the Devonian sediments, metamorphosed Habahe Group metasediments, migmatites, and the granitoids [after Jiang *et al.*, 2015]. Vertical axis not to scale. (b) Field photographs illustrating progressive increase in melting degree toward the granitoid. Localities of representative samples are shown on the profile above. (1) Garnet-sillimanite paragneiss. Metamorphic zircons from this unit have ages of ~389 Ma [Jiang *et al.*, 2010]. (2–4) Progressive textural evolution of migmatite types toward the granitoid, from ophthalmitic gneiss, through stromatolites, to nebulites. The insert shows a rare kyanite relic preserved in the migmatite. (5) Garnet- and muscovite-bearing leucogranite. (6) Oriented biotite and hornblende define a strong L fabric in granitoid batholith. The indicated formation age of the granitoid from Yuan *et al.* [2007].

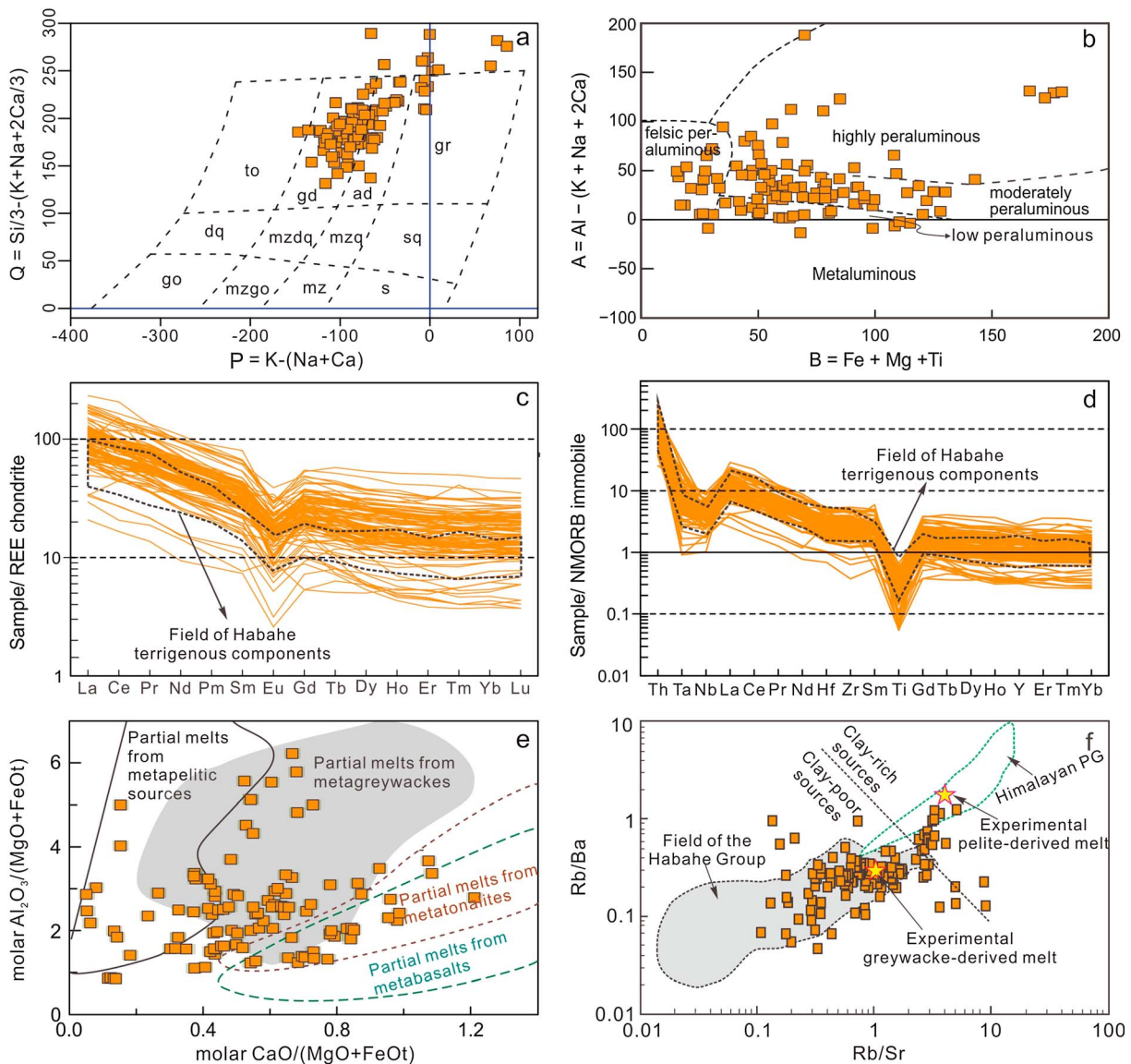


Figure 6. Geochemical characteristics of Silurian-Devonian granitoids and felsic volcanic rocks ($\text{SiO}_2 > 65 \text{ wt } \%$) from the Chinese Altai. (a) Classification of granitoids and related rocks after *Debon and Le Fort* [1983]. (b) B-A diagram of *Villaseca et al.* [1998] modified from *Debon and Le Fort* [1983] showing that granitoids from the Chinese Altai are characterized by predominantly peraluminous compositions. (c) Chondrite-normalized REE and (d) N-MORB normalized trace element patterns for granitoids and felsic volcanic rocks. Field of the Habahe Group terrigenous component is also shown for comparison. Chondrite and N-MORB normalizing values are from *Sun and McDonough* [1989]. (e) Binary plot ($\text{CaO}/(\text{MgO} + \text{FeO}_t)$ versus $\text{Al}_2\text{O}_3/(\text{MgO} + \text{FeO}_t)$ (mol %) after *Gerdes et al.* [2002] to distinguish granitic melts derived from various crustal sources. (f) Plots of Rb/Sr versus Rb/Ba after *Sylvester* [1998] to constrain the possible origin of the Altai granitoids. Fields of the Habahe Group rocks (including volcanogenic and terrigenous components) and the Himalayan peraluminous granites (Himalayan PG) are also shown for comparisons. Details on data sources are available in the supporting information S1, and related data are presented in Table S1. Plotting was done by the *GCDKit* package of *Janoušek et al.* [2006].

($\epsilon_{\text{Nd}}(400\text{Ma}) = +10$ and $\text{Nd} = 3.6 \text{ ppm}$) was also tested (hyperbola A'-B in Figure 7a). For such a mixing model, the required proportions of the basic components are unrealistically high ($> 80\%$, Figure 7a). If the average composition of the Habahe Group terrigenous rocks ($\epsilon_{\text{Nd}}(400\text{Ma}) = -3.7$, $\text{Nd} = 28.4 \text{ ppm}$, point C in Figure 7a) is used as the crustal end-member in the calculation, then much less proportion of the primitive basaltic component would be needed (0–60 wt %, Figure 7a). Nevertheless, compared with the terrigenous components of the Habahe Group, a minor group of granitoids (~15%) tend to have less evolved Nd isotopic characteristics with the initial ϵ_{Nd} values ranging from +1 to +6 (Figure 7a), implying an involvement of a primitive component with a rather radiogenic Nd isotopic character.

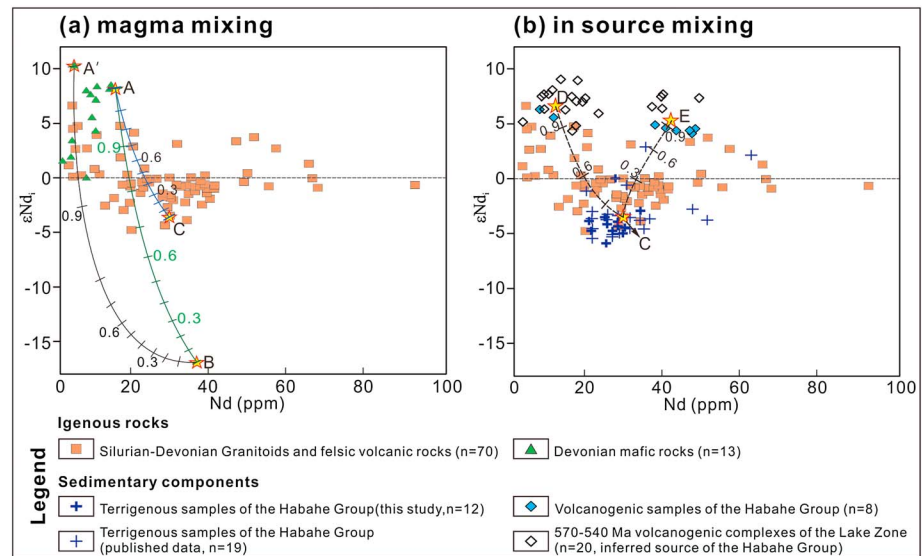


Figure 7. Nd isotopic diagrams for (a) felsic igneous (including granitoids and their eruptive equivalents) and mafic rocks from the Chinese Altai and (b) the Habahe Group terrigenous and volcanogenic rocks in the Chinese Altai and the volcanogenic complexes from the Lake Zone in western Mongolia. (a) Mixing hyperbolae from the previous studies, i.e., magma mixing (invoking the hypothetical Precambrian basement: curve A-B [after Jahn *et al.*, 2004; Wang *et al.*, 2009]) and with the lowest Nd basalt as the mantle end-member (A'-B) were superimposed using the R code of Janoušek *et al.* [2016]. Proportions of the juvenile depleted mantle-derived end-member are indicated (tick marks interval is 10%). (b) Two possible hyperbolae for binary mixing in the Ordovician Habahe Group (i.e., in source mixing) between the average terrigenous component ("C," Figure 7b) and two volcanogenic end-members with contrasting Nd concentrations (i.e., "D": Nd ($\epsilon_{Nd}(400\text{Ma})=+6.8$ and Nd=12.4 ppm and "E": Nd ($\epsilon_{Nd}(400\text{Ma})=+5.4$ and Nd=40.9 ppm, Figure 7b). Proportions of the volcanogenic components are indicated (tick marks interval is 30%). Further explanations in text. Details on data sources are available in the supporting information S1, and related data are presented in Table S3.

In any case, the results of the simple binary mixing model should be taken only as a guide in evaluation of approximate amount of the basaltic component, since the nature of the real depleted mantle end-member could be different. However, we can tentatively conclude that the required proportion of the basaltic component may have been previously overestimated, especially if the Habahe Group rocks replace the hypothetical Precambrian basement in the calculations.

In reality, two scenarios can be envisaged. The required primitive component could have been added by *magma mixing* with depleted mantle-derived basaltic melts, as suggested in previous studies [e.g., Wang *et al.*, 2009]. However, such a simplistic model may be at odds with the strikingly different physical properties of basic and acid liquids (e.g., their great viscosity contrast) and the available geological data as will be discussed in more detail later. Alternatively, the primitive component could have been already present in the crustal magma source in the form of basic volcanic admixture or tuffitic layers (in source mixing). It is noteworthy that the Habahe Group indeed does contain a significant amount of intermediate to mafic volcanogenic components [Windley *et al.*, 2002], which were considered to be derived from Neoproterozoic oceanic arc-related complexes in western Mongolia, particularly from the Lake Zone (Figure 2) [see also Long *et al.*, 2008; Jiang *et al.*, 2011].

Neodymium isotopic data of volcanogenic components from six amphibolite layers of the Habahe Group and 20 volcanic-volcanoclastic rocks of the Lake Zone were collected from previously published work [Hu *et al.*, 2000; Kovach *et al.*, 2011], in order to evaluate the possible contribution of Early Paleozoic volcanogenic component on the isotopic signature of the Habahe Group. Their ϵ_{Nd} (400Ma) values vary in a range of +4–+6.3 and +4.3–+9.0, respectively, broadly falling into two groups in terms of their Nd abundances (Figure 7b), and are thus hard to distinguish from the variably depleted mantle-derived magmas (Figure 7b and Table S3). This is consistent with the widely accepted view that the Habahe Group contains abundant geochemically primitive components [Cai *et al.*, 2011a; Liu *et al.*, 2012; Long *et al.*, 2012]. Clearly, the Nd isotopic signatures of nearly all granitoids can be attained by mixing in the source of these two components in various proportions (Figure 7b). It is therefore possible to envisage that the presence of basic volcanic admixture or tuffitic layers

in the magma source would significantly lower the required contribution of the mantle-derived magmas, often perhaps down to nil.

Such a model can be tested by the Rb-Sr-Ba variations in the Habahe Group rocks and the studied granitoids. It has been suggested that partial melting of greywacke-like immature sediments, i.e., the Habahe Group in our case, would leave behind large amounts of plagioclase [e.g., *Montel and Vielzeuf, 1997*]. Because Sr and Ba are compatible in plagioclase, whereas Rb is incompatible [e.g., *Harris and Inger, 1992*], melts derived from such sources will tend to have higher Rb/Sr and Rb/Ba than their sources [*Sylvester, 1998*]. This is in good agreement with the fact that the studied granitoids have systematically higher Rb/Sr and Rb/Ba ratios than their prospective sources, i.e., the Habahe Group (Figure 6f).

Taken together, the partial melting of the Habahe Group rocks could have produced the bulk of the parental magma to the studied Silurian-Devonian granitoids, while the required depleted mantle contribution could have been considerably less than that proposed by other authors [e.g., *Wang et al., 2009*].

3.2. Thermodynamic Modeling of Partial Melting of the Habahe Group Terrigenous Metasediments

It has been shown that the Habahe metasediments were buried to deep crustal levels (>30 km) where they underwent extensive anatexis (Figure 4) [*Jiang et al., 2015*]. Based on available petrological observations, a remarkably high metamorphic gradient of ~30°C/km (Figure 4) can be inferred from the Devonian metamorphic fabrics. Such a high gradient has been equally inferred by lines of geological evidence as will be discussed in more detail later. It is therefore feasible to envisage that the anatexis reworking the deep orogenic crust (30–40 km) could attain temperature close to 1000°C. In order to investigate the partial melt compositions, the composition of the dominant Habahe Group terrigenous metasediments was used to model at *P-T* conditions of 8–12 kbar, 800–1100°C (Figure 8a) using the Perple_X software [*Connolly, 2005*]. The amount of H₂O was set to just allow a H₂O-saturated solidus which allows the modeling of partial melting process in a H₂O-closed system. Details on thermodynamic modeling are available in the supporting information S1. Representative compositions of melts that are in equilibrium with garnet- and/or orthopyroxene-bearing assemblage in a *P-T* range corresponding to anatectic conditions are computed directly via the Perple_X software. Values of oxides have been normalized to 100% on an anhydrous basis and then plotted in Figures 8b–8d and presented in Table 1.

Major features of the pseudosection are biotite dehydration melting around 830°C and stabilization of garnet and garnet pyroxene-bearing assemblages at higher temperature conditions. The result shows that the Habahe terrigenous metasediments are sufficiently fertile to produce large volumes of melt, for example, from 5 vol % melt at 800°C to >50 vol % melt at 1000°C (Figure 8a). Predicted is progressive disappearance of biotite, K-feldspar, garnet, and plagioclase, contemporaneous with systematic decrease of K₂O and increase of CaO and MgO contents in the melt with increasing temperature (Figure 8b). It is shown that the major element composition of the resultant melt mainly depends on the temperature. The calculated melt compositions are comparable to those of experimental metagreywackes-derived melts under similar *P-T* conditions (Figure S1). In general, the modeled melts have granite to granodiorite compositions, similar to most granitoids and felsic volcanic rocks in the region (Figure 8c).

However, there remains a minor group (~15%) of granitoids that have tonalitic compositions, characterized by lower SiO₂, and higher CaO and MgO contents, compared to the modeled melts (e.g., Figure 8d). This suggests that a certain addition of more basic component must have been also involved in the petrogenesis of the granitoids. As we discussed above, this could have been realized either via magma mixing with mantle-derived mafic magmas or via partial melting of a mafic protolith, such as the volcanogenic components of the Habahe Group. Due to lack of an appropriate melt model for basic rocks in the Perple_X software, melt compositions from partial melting of these volcanogenic components cannot be currently modeled. However, as demonstrated by experimental studies, tonalitic melts can be produced by partial melting of metabasic rocks [*Rapp and Watson, 1995; Skjerlie and Patiño Douce, 1995; Green et al., 2016*]. Data from melting experiments at 850–1000°C/10 kbar, of a quartz amphibolite [*Patiño Douce and Beard, 1995*] and a calcic amphibolite [*Wolf and Wyllie, 1994*], were plotted in Figures 8b and 8c, and they show high CaO and MgO contents. It is therefore possible to envisage that partial melting of the Habahe Group volcanogenic components at these *P-T* conditions may have produced compositionally similar melts and thus may be responsible for the origin of the subordinate CaO and MgO rich granitoids.

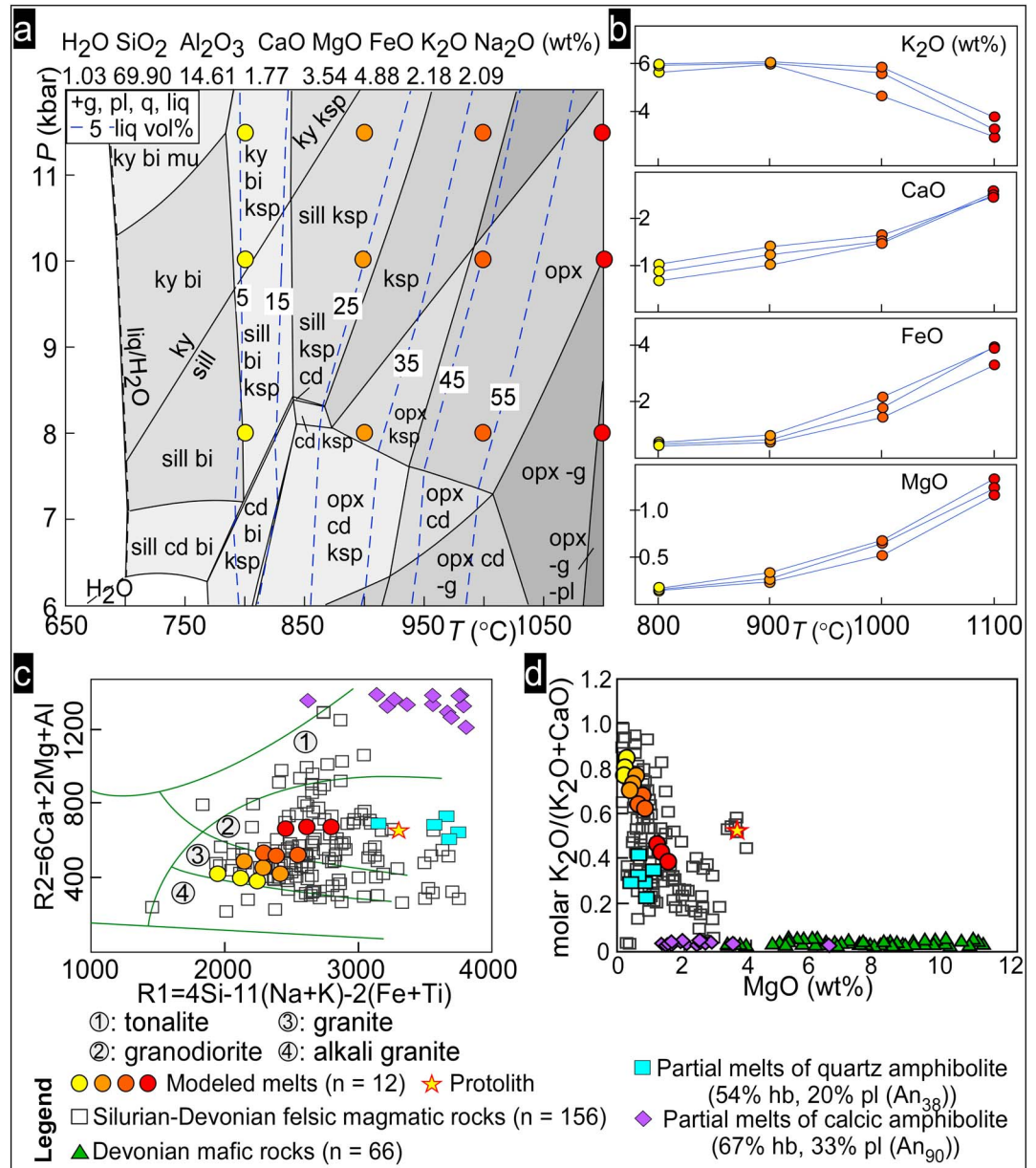


Figure 8. (a) *P-T* pseudosection for the average Habahe Group metasediments with calculated melt proportion isopleths. *P-T* conditions of the modeled melts are indicated by filled squares. (b) Contents of representative oxides plotted versus temperature. (c) Multicationic diagram R_1-R_2 [De La Roche *et al.*, 1980] with modeled melts and Silurian-Devonian felsic magmatic rocks of the Chinese Altai. The average Habahe composition is indicated by a star. (d) Whole-rock chemical projection for modeled melts and felsic and mafic rocks of the Chinese Altai. Compositions of partial melts from melting experiments of a quartz amphibolite [Patiño Douce and Beard, 1995] and of a calcic amphibolite [Wolf and Wyllie, 1994] are shown for comparison and presented in Table S4.

It should be noted that modeled melt compositions provide only constraints on the nature of the liquids. However, most granitoids are not simple partial melts but rather complex solid-liquid suspensions. For instance, from their source region they may bring entrained mafic and felsic restite phases [e.g., Clemens and Stevens, 2012] and on the way to the surface they undergo a variety of physical and chemical processes and interactions, including assimilation, fractional crystallization, and crystal accumulation. This may alternatively explain larger variation in chemistry of the granitoids compared to the modeled partial melt compositions.

Table 1. Compositions of Modeled Melts From Partial Melting of the Habahe Group Terrigenous Component (Normalized to 100wt % Anhydrous)

Melt	P-T (kbar/°C)	Residue Assemblage	SiO ₂	Al ₂ O ₃	CaO	MgO	FeO	K ₂ O	Na ₂ O
1	11.5/800	g ky bi ksp pl q	72.78	15.71	0.84	0.14	0.47	5.98	4.08
2	11.5/900	g sill ksp pl q	72.09	16.45	1.21	0.23	0.57	6.14	3.30
3	11.5/1000	g ksp pl q	71.24	16.55	1.46	0.52	1.45	5.82	2.96
4	11.5/1100	g opx pl q	68.80	17.53	2.29	1.17	3.29	3.69	3.23
5	10/800	g ky bi ksp pl q	73.37	15.52	0.69	0.15	0.48	5.89	3.90
6	10/900	g sill ksp pl q	72.47	16.33	1.04	0.27	0.66	6.11	3.13
7	10/1000	g opx pl q	71.47	16.24	1.32	0.65	1.80	5.59	2.93
8	10/1100	g opx pl q	67.68	18.72	2.34	1.25	3.94	3.15	2.92
9	8/800	g bi sill ksp pl q	74.05	15.22	0.51	0.16	0.58	5.73	3.74
10	8/900	g opx ksp pl q	72.97	16.03	0.84	0.34	0.85	6.06	2.91
11	8/1000	g opx pl q	70.63	17.69	1.28	0.68	2.20	4.61	2.91
12	8/1100	opx pl	68.85	17.92	2.33	1.35	3.96	2.86	2.74

4. Partial Melting of the Habahe Group Rocks and Its Effect on the Composition and the Density of the Chinese Altai Lower Crust

In this part, the densities of both molten and unmolten Habahe Group terrigenous metasediments are thermodynamically modeled and discussed in the frame of a gravity model of the Altai Mountains.

4.1. Thermodynamic Modeling of Lower Crustal Composition and Density

The extensive partial melting of the Habahe Group metasediments would lead to large-scale differentiation of the crust through extraction and ascent of felsic melt to middle and upper crustal levels, leaving a dense and refractory lower crust. The mineral assemblages and corresponding density of such residue can be modeled using a pseudosection approach.

To estimate physical characteristics of the lower crust with such a thermal gradient, a reference point of 9kbar (approximately 35km depth) and 950°C is used (Figure 8a), on the basis of the calculated metamorphic field gradient of ~30°C/km (Figure 4). At these conditions, calculated equilibria for average Habahe Group terrigenous metasediment show granulite-facies mineral assemblage g-opx-ksp-pl-q in equilibrium with ~35vol % of melt (Figure 8a). It is supposed that in the crust most melt would migrate up and would be lost from the granulite. Therefore, 90% of melt was extracted from the modeled system and the bulk chemical composition of the residue was used to calculate a new pseudosection contoured for density (Figure 9).

The resulting pseudosection has a high solidus temperature (~850°C) due to limited melt and hence H₂O contents. Garnet is stable throughout the whole calculated range, and orthopyroxene occurs mainly in supersolidus conditions. In general, the densities of the residue increase from melt-bearing to melt-absent assemblages varying from about 2840kg/m³ at 1000°C to about 2890kg/m³ at 750°C (Figure 9a). The residue at 9kbar and 950°C would have garnet-orthopyroxene-bearing granulite-facies assemblage, characterized by a high garnet fraction (22.3vol %) with density of 2858kg/m³ ("a" in Figure 9a). Cooling of such a residue would cause approximately 1% increase of the rock density for a temperature interval of ~200°C (Figure 9a). Partial melting of subordinate volcanogenic components with presumably andesitic-basaltic compositions in deep crust would also leave behind a dense residue rich in garnet and pyroxene [e.g., Patiño Douce and Beard, 1995; Hartel and Pattison, 1996; Guy et al., 2015; Green et al., 2016]. In conclusion, a high-density residue would be left after anatexis of the Habahe Group metasediments in the lower crust, and the resulting density would be very different from that of the metasediments that did not experience anatexis.

Ordovician metasediments similar to the Habahe Group also occur in the neighboring Hovd-Mongolian Altai Zone and are metamorphosed at greenschist to amphibolite-facies conditions [Badarch et al., 2002]. The metamorphic assemblages and densities of such rocks can be inferred from modeling of the Habahe Group rocks in subsolidus conditions (Figure 9b). The pseudosection shows classical metapelite greenschist and amphibolite-facies assemblages with density variation mainly between 2680 and 2830kg/m³ in a pressure range of 3–10kbar, corresponding to depths of 10–40km. Considering a moderate metamorphic gradient of ~20°C/km as inferred from the regional amphibolite-facies assemblages from the Chinese Altai [Wei et al., 2007; Jiang et al., 2015], the rocks in the lower crust at ~35km could reach ~700°C. At these

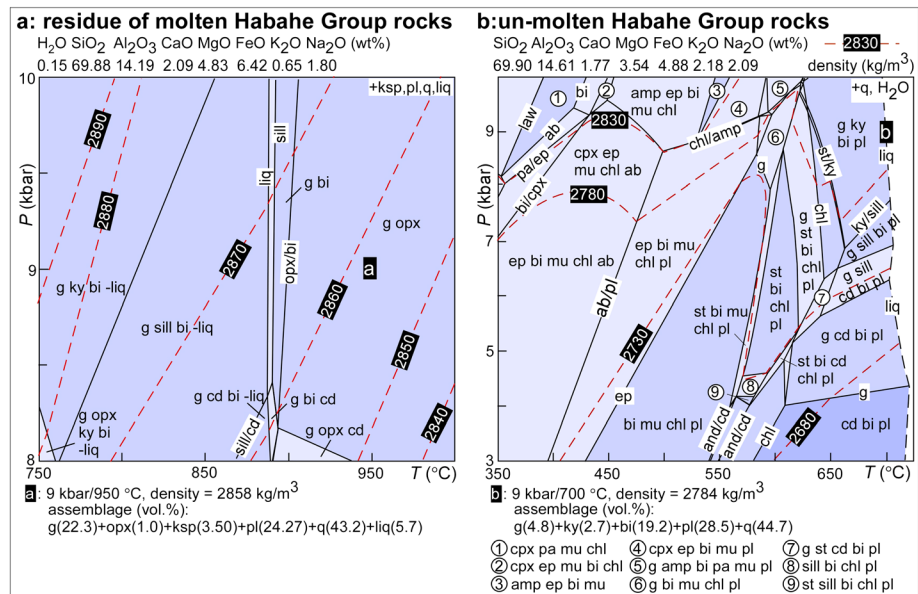


Figure 9. (a) *P-T* diagram showing residue assemblages and resulting densities after melt extraction for the molten Habahe Group rocks. (b) *P-T* diagram for the average Habahe Group metasediments showing mineral assemblages and density for subsolidus conditions.

conditions, the Habahe Group rocks would have garnet-kyanite-staurolite-bearing metamorphic assemblages with density around 2780 kg/m³ (Figure 9b), i.e., a density significantly lower than the modeled granulite-facies assemblage in the lower crust of the Chinese Altai.

4.2. Residual Gravity High Over the Chinese Altai: A Consequence of Crustal Anatexis?

After the Devonian period, the Chinese and Mongolian Altai did not experience any prominent magmatism and further crustal differentiation. Therefore, the lateral differences in their lower crustal densities resulting from contrasting Devonian metamorphic conditions should be preserved. To test it, the analysis of gravity signal of the crust was performed. The Complete Bouguer anomalies range from -216 mGal to -6 mGal and reveal two principal domains (Figure 10a): (1) a large-scale gravity low corresponding to the Mongolian Altai and Hovd (MA-HVD) regions in the NE half segment and (2) a large-scale gravity high corresponding to the Chinese Altai and the Junggar Basin in the SW half segment. The Bouguer anomaly map still contains the long-wavelength signals of the crust-mantle boundary and the upper mantle, which tend to conceal the shorter-wavelength signals. Consequently, the isostatic residual Bouguer gravity anomaly map has been computed from the Complete Bouguer gravity anomalies from the World Gravity Map 2012 model [Balmino *et al.*, 2012] using the Airy-Heiskanen compensation model [Heiskanen and Moritz, 1967] with the depth of the compensating root of 30 km at sea level in areas of no topography, a density contrast across the Moho of 330 kg/m³ [Hinze *et al.*, 2013], and a density of the crustal topography of 2670 kg/m³ (Figure 10b). Thus, the long-wavelength anomalies are removed from the gravity signal and the variation of the densities in the crust can be analyzed for the Chinese Altai, its neighboring MA-HVD region, and the northern Junggar Basin. The resultant residual gravity anomalies are different among these three regions, still marked by gravity low for the Mongolian Altai to the north (MA-HVD in Figure 10), but the Chinese Altai reveals gravity anomaly high, whereas the Junggar displays an intermediate gravity signal (Figure 10b). Therefore, the pronounced long-wavelength residual gravity high in the Chinese Altai suggests a relatively denser lower crust compared to the adjacent MA-HVD and Junggar Basin regions.

The question of whether the gravity anomalies across the Altai Orogenic Belt can be linked with the metamorphic evolution is further investigated by conducting a forward gravity modeling of the Complete Bouguer anomalies along a selected profile (Figure 10c). In the absence of any seismic profile across the Chinese Altai and MA-HVD regions, the modeling of the crust-mantle boundary is constrained by the CRUST 1.0 model [Laske *et al.*, 2013] combined with the seismic profiles of Zhao *et al.* [2003] and Wang *et al.* [2003] for the Junggar Basin. In addition, the gravity modeling is constrained by surface geological

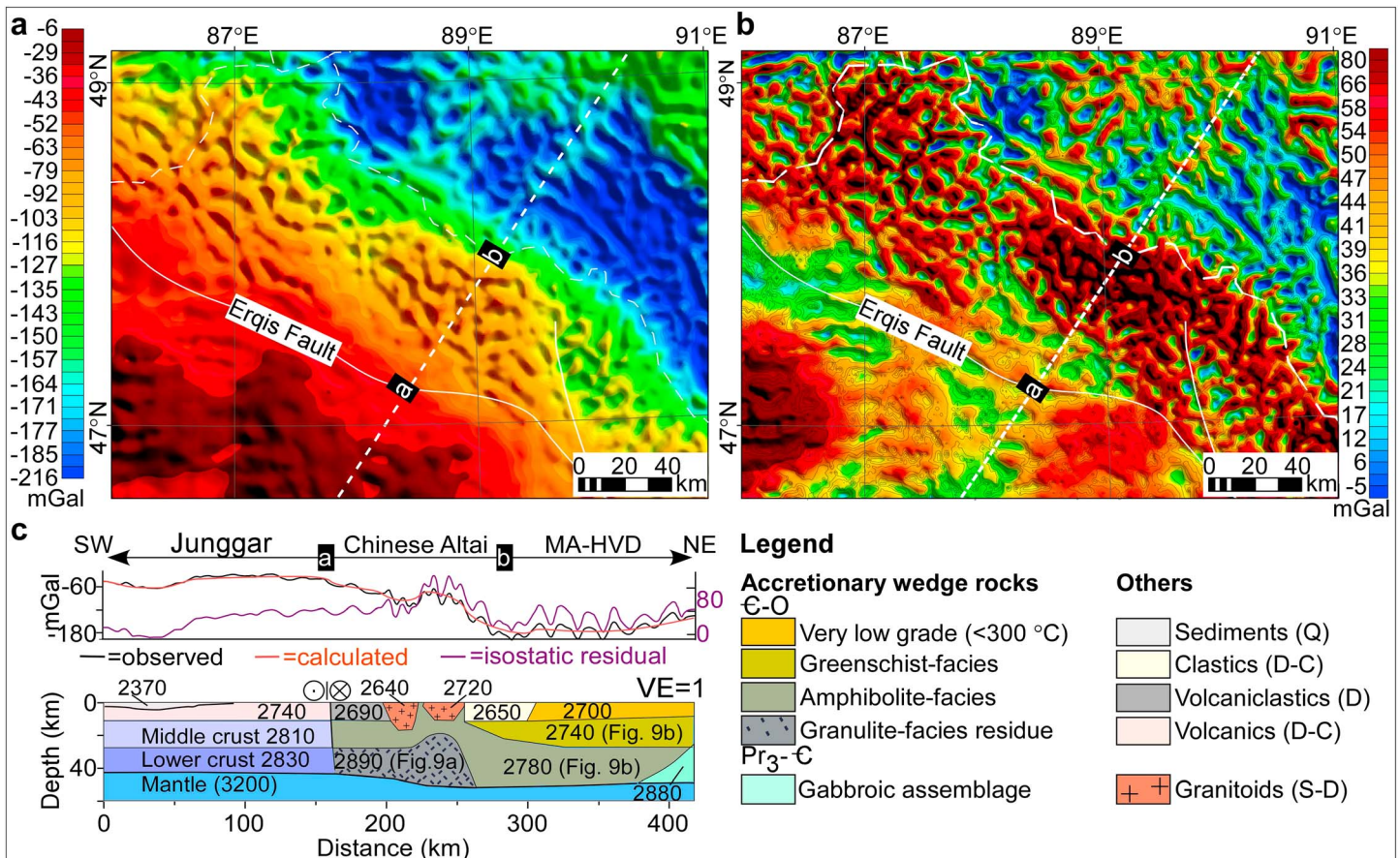


Figure 10. (a) Complete Bouguer gravity anomaly map of the Chinese Altai and adjacent regions. (b) Isostatic residual Bouguer gravity anomaly map. The white lines correspond to the Ergis and Fuyun fault zones inferred from the surface geology. (c) Gravity model across the Altai orogen showing the possible source of the gravity anomalies. VE: vertical exaggeration.

observations and the boundaries of the major lithological units. In this profile, the crustal architecture of the Junggar portion was constrained by available geological and seismic data of *Zhao et al.* [2003] and *Bian et al.* [2010]. The Chinese Altai architecture featured by doming of dense lower crustal rocks was inferred from *Jiang et al.* [2015], and the MA-HVD structure was characterized by Mongolian Altai Ordovician metasediments thrust over the Early Cambrian gabbroic rocks of the Lake Zone based on the study of *Lehmann et al.* [2010]. The density (2890 kg/m³) of the modeled residue from a depth of approximately 35 km (9 kbar) was taken as the best estimation for the average density of the lower crust of the Chinese Altai. Given the widely exposed amphibolite-facies rocks in the Chinese Altai, the density of 2780 kg/m³, corresponding to the Habahe Group metasediments under the amphibolite-facies condition (Figure 9b), was assigned as the average density estimation for the middle crust of the Chinese Altai. The densities of the lower and middle crust of the MA-HVD region were taken from the modeling of the Habahe Group terrigenous metasediments under amphibolite- and greenschist-facies, with densities of approximately 2780 kg/m³ (9 kbar/700°C, Figure 9b) and 2740 kg/m³ (5 kbar/450°C, Figure 9b), respectively. The densities of other lithological units come from general rock densities of *Telford et al.* [1990] based on their respective petrological features and keeping the most realistic density contrasts between the different units.

During the modeling, the intermediate- to short-wavelength gravity anomalies corresponding to the isostatic residual Bouguer anomalies were first modeled, in order to constrain the geometry of the density units. The Complete Bouguer anomalies that contain signals of the long wavelength were appended thereafter, in order to adjust the densities of the lower crustal signal. Following these steps, the modeled long-wavelength Bouguer gravity anomalies provide a good match with the observed one (Figure 10c). It therefore proves that the emplacement of a dense granulite residue under the Chinese Altai can provide the observed high gravity signal. The

presence of a dense lower crust under the Chinese Altai was previously determined from a density model inferred from seismic data [Zhao *et al.*, 2003], and it was thought to be caused by mafic-ultramafic cumulates crystallized from the ascending arc magma. However, the density values used in their model for the lower crust of the Chinese Altai range from 2970 to 2990 kg/m³, significantly higher compared to our model. Alternatively, the results from this work provide a yet not considered explanation for contrasting gravity features across the Altai Orogenic Belt which links with different metamorphic evolution of the Chinese Altai and MA-HVD.

It should be emphasized that the forward gravity modeling is a quantitative method and thus the modeling results are nonunique. However, the ambiguities about the nature of the dense lower crust could be reduced significantly when the modeling is constrained using geological observations (Figure 5), combined with metamorphic petrology (Figure 4), geochemistry (Figures 6 and 7), and geophysical data (Figure 10).

5. Discussion

5.1. Crustal Architecture of the Chinese Altai

The Chinese Altai has been classically considered as a continental unit represented by a Precambrian basement covered by Ordovician to Carboniferous sediments [Windley *et al.*, 2002]. Based on such assumption, the calc-alkaline granitoids with hybrid crust-mantle geochemistry (Figures 6a–6e) were exclusively interpreted as the products of a Cordilleran-type continental arc magmatism [Wang *et al.*, 2006, 2009]. This assumption seems to fit with the presence of a high seismic *P* wave velocity layer (6.9–7.0 km/s, *P* wave velocity) in the lower crust that was interpreted as composed mainly of amphibolite, mafic granulite, and subordinate metadiorite and metatonalite [Wang *et al.*, 2003]. Such a mafic to ultramafic lower crustal composition can be a vestige of massive basic magma underplating [e.g., Artemieva and Meissner, 2012]. However, the isotopic signal of the “enigmatic” basement can be only a reflection of a “ghost” signal from inherited detrital sediments derived from the Tuva-Mongolian Continent which contributed to Precambrian detritus to the Ordovician accretionary wedge [Sun *et al.*, 2008; Jiang *et al.*, 2011]. Moreover, the Chinese Altai granitoids form isolated circular or elongated bodies, spatially disconnected from subordinate gabbroic intrusions, which is not compatible with typical Cordilleran-type continental arcs typified by continuous diorite-tonalite-granodiorite coastal batholiths rich in variously hybrid mafic components [e.g., Ducea *et al.*, 2003]. Indeed, some recent studies suggested that the Chinese Altai can be regarded as a segment of a giant Early Paleozoic accretionary system extending from western Mongolia to Chinese Altai consisting exclusively of greywacke-dominated Ordovician sediments [Xiao *et al.*, 2009; Long *et al.*, 2010]. Such an interpretation suggests a crustal architecture distinctly different from the traditional geotectonic model of the Chinese Altai and calls also for a reevaluation of the current ideas on the granitoid petrogenesis.

The exhumed orogenic lower crustal sections are well exposed in cores of high-grade migmatite-magmatite domes in both the Chinese and Mongolian Altai [Jiang *et al.*, 2012, 2015; Broussolle *et al.*, 2015; Zhang *et al.*, 2015]. These crustal sections are exclusively composed of metamorphosed Habahe-type metasedimentary sequence without any fragments of old continental basement and gabbroic intrusions (Figure 11a). The rocks resembling a melt-stripped residue modeled in the current study were so far retrieved from rare orthopyroxene-bearing granulite lenses in migmatites [Kozakov *et al.*, 2002; Wei *et al.*, 2007] and two-pyroxene granulite xenoliths sampled by Mesozoic volcanic rocks in Mongolian Altai [Barry *et al.*, 2003]. These xenoliths show predominantly crust-like evolved Sr-Nd isotopic characteristics similar to the Habahe Group (Figure 11) and (garnet)-pyroxene-bearing assemblages, which are comparable to the modeled granulitic residue resulting from the partial melting of the Habahe Group metasediments. It is noteworthy that the high-grade domes are cored by felsic granitoids that are compositionally and isotopically comparable to the hosting Habahe Group metasedimentary rocks (Figure 11a).

Such a rock association is not compatible with the traditional petrogenetic model, which assumes partially molten old basement intruded by basic magmas in the deeper crustal sections as reported from the European Variscan Belt [e.g., Soula *et al.*, 1986; Aguilar *et al.*, 2015]. This orogenic belt is a classic example of such a thermal and magmatic reworking of an old (Proterozoic) continental basement during Late Carboniferous to Permian lithospheric thinning [e.g., Ziegler, 1986; Artemieva and Meissner, 2012]. This event resulted in production of voluminous basaltic magmas triggering melting of the overlying basement and production of mixed calc-alkaline magmas (e.g., in Corsica and Pyrenees [Rossi and Cocherie, 1991; Roberts *et al.*, 2000]). The resulting crustal structure is marked by mafic lower crust overlain by intermediate

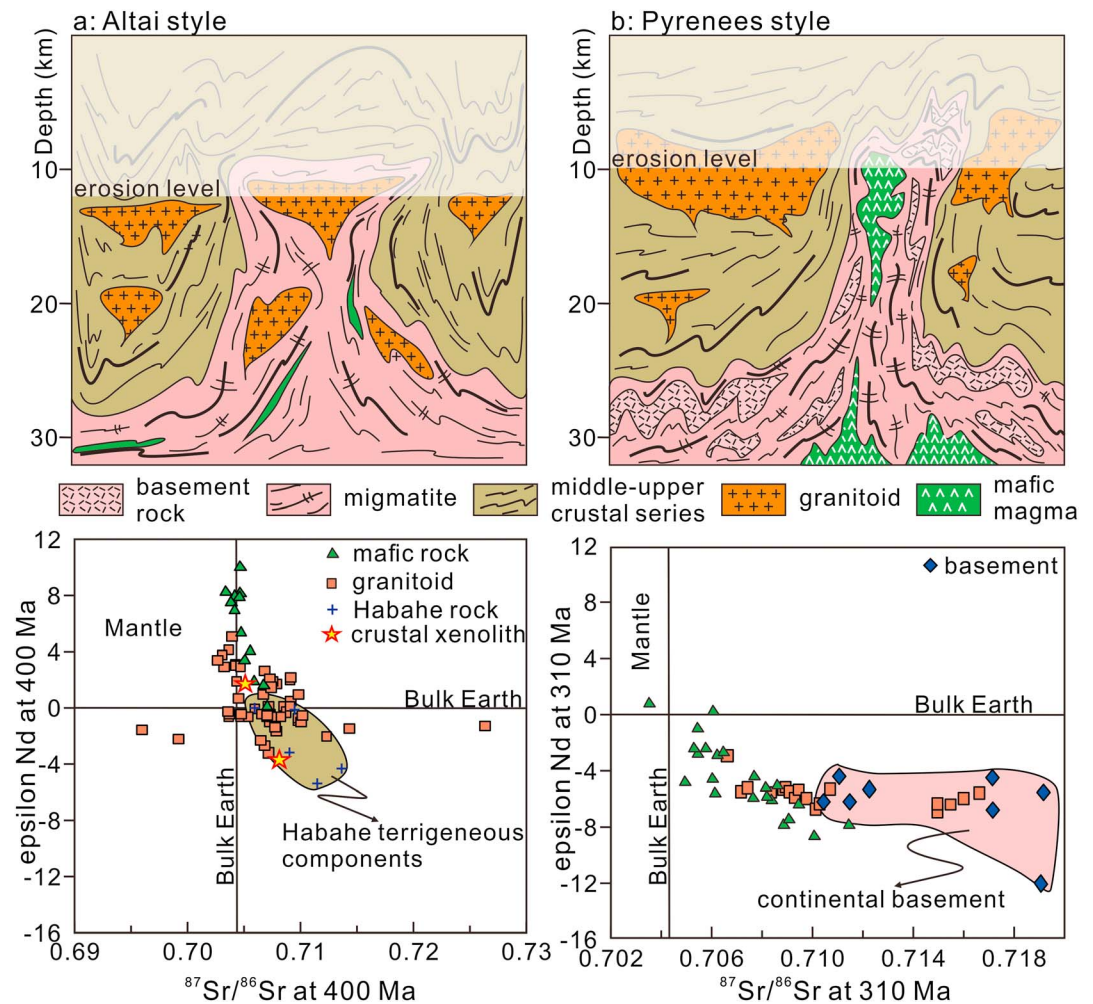


Figure 11. Granitoid petrogenesis and orogenic crustal architecture of (a) the Altai-type orogen (modified after Jiang *et al.* [2015]) and (b) the Pyrenees-type orogen (modified after Aguilar *et al.* [2015]). Figure 11a shows anatectic melting of thickened sedimentary sequences generates ascending granitoids. The contribution of juvenile mantle-derived magma is limited. Figure 11b shows intense interaction between mantle-derived magmas and continental basement with important input of mantle components. Isotopic data for the Chinese Altai orogen are after Hu *et al.* [2000] and Wang *et al.* [2009, and references therein], data for crustal xenoliths are from the Mongolian Altai after Barry *et al.* [2003], and those of European Variscides are after Bickle *et al.* [1988], Roberts *et al.* [2000], and Vilà *et al.* [2005]. Summary of data are presented in Table S5.

to felsic granulites and by metasedimentary middle to upper crust [Downes, 1993; Rey *et al.*, 1997; Artemieva and Meissner, 2012]. Taken the Pyrenees as an example, the exposed deeper crust in the core of Late Carboniferous gneiss domes features locally granulitic and partially molten Precambrian basement associated with tonalite-granodiorite plutons and massive syntectonic gabbro-diorite injections [Druguet, 2001; Aguilar *et al.*, 2015]. The mantle-derived magmas there generally show evolved Sr-Nd isotopic signatures exemplified by their mostly negative $\epsilon_{Nd}(t)$ values, a few of which are even less radiogenic than the basement (Figure 11b). The isotopic signatures of the Pyrenean granodiorites are overlapping largely with those of the basement and mantle-derived mafic rocks, and this can be explained by magma mixing between mantle- and basement-derived magmas (Figure 11b).

In our view, the crustal architecture of the Altai Orogen is likely represented, from the bottom to the top, by intermediate granulites, migmatites, and amphibolite- to greenschist-facies metasediments all derived from the Habahe Group and such a package is intruded by granitoids mainly of granitic to granodioritic composition. Contrary to the Pyrenees example, the absence of mafic intrusions in the exposed lower crustal section in the Chinese Altai migmatite-magmatite domes precludes supposed large-scale mantle-derived magma underplating.

5.2. Habahe Group Rocks as a Source of Altai Granitoids

As shown above, the Silurian-Devonian calc-alkaline granitoids in the Chinese Altai are characterized by hybrid crust-mantle geochemistry and variable initial Sr-Nd isotopic compositions (Figure 7) [see also *Chen and Jahn, 2002; Wang et al., 2009; Liu et al., 2012*]. They are also depleted in HFSE and enriched in LILE on the N-MORB normalized spidergrams (Figure 6d). Such geochemical features suggest that they either represent fractionation products of typical continental arc-derived magmas or they came from magmatic recycling of young, geochemically immature arc-derived sediments [*Arculus, 2003; Janoušek et al., 2010*]. The latter scenario has rarely been considered until geochemical similarities were found between granitoids and the Habahe Group rocks, implying that the latter may have contributed to the magma source in the Chinese Altai [*Liu et al., 2012*].

The commonly positive zircon $\epsilon_{\text{Hf}}(t)$ values and relatively primitive whole-rock Sr-Nd isotopic characteristics of the granitoids were interpreted as due to the involvement of significant amount of primitive basic component (70–90%) in the magma [e.g., *Wang et al., 2009*]. Such model requires a presence of an old continent and large amount of basic and intermediate cumulates [*Borg and Clynne, 1998*]. However, such a scenario of significant mantle-crust interaction is apparently at odds with the available petrological and geochemical data: (1) most granitoids have high SiO₂ (65 to 78wt %) and low MgO (2% to <0.1wt %), high-K or normal calc-alkaline, peraluminous compositions [*Liu et al., 2012*]; (2) the mafic microgranular enclaves in granitoids as well as contemporaneous mafic intrusions are relatively rare in the exposed lower crustal section (Figure 11a); and (3) the relatively high Nd abundances of the granitoids preclude a large participation of depleted mantle-derived mafic magmas.

On the contrary, the following lines of evidence support magmatic recycling of the Habahe Group rocks: (1) the reconstructed crustal profile shows that these rocks were buried into deep crustal levels where they underwent extensive anatexis [*Jiang et al., 2015*]; (2) there is a temporal and spatial relationship between the anatexis of the Habahe Group rocks and formation/emplacement of the granitoids (Figure 5); (3) thermodynamic modeling shows that the Ordovician metasediments are fertile enough to produce large volumes of granitic to granodioritic melts resembling most granitoids in the Chinese Altai (Figure 8); and (4) partial melting of both volcanogenic and terrigenous components of the Habahe Group could produce melts isotopically identical to the granitoids (Figure 7). In fact, the compositions of granitoids as well as their origin proposed in this work match well the classic S-type granites in circum-Pacific orogens, as exemplified by *Collins and Richards [2008]*.

Based on these data, an updated petrogenetic model for the Altai granitoids is proposed. The predominant (~85 vol %) peraluminous granitoids (biotite granodiorites to granites) could have originated mainly by partial melting of the greywacke-like Habahe Group metasediments (Figure 12). The remaining (~15 vol %) relatively Ca-Mg rich "I-type" hornblende tonalites to granodiorites could have resulted from partial melting of volcanogenic components of the Habahe Group (Figure 12). The resultant granitoids could share arc-like isotopic and trace element signatures reflecting inheritance from the Habahe Group (Figure 12). Similar granitoids derived from flyschoid sediments in accretionary prisms commonly show I-type geochemical characters and arc-like affinities (e.g., in Alaska) [*Barker et al., 1992*]. However, like in the Altai, their geochemical features only reflect the source rocks rather than the true tectonic environment of origin. Considering the contemporary emplacement of minor mafic rocks, magma mixing with mantle-derived component could also be a feasible possibility for the generation of these minor hornblende-bearing granodiorites. Taken together, the primitive geochemical characteristics of the granitoids could be mostly inherited from isotopically unevolved Habahe Group rocks and the contribution of primitive basic component could have been significantly less than previously proposed.

5.3. Implications for the Crustal Evolution of the CAOB and Peripheral Continental Growth in General

Accretionary processes in northern Mongolian CAOB are characterized by the general southwestward oceanic evolution successively from Late Neoproterozoic to Early Paleozoic [*Badarch et al., 2002; Kröner et al., 2010; Lehmann et al., 2010*]. Recent studies have suggested that this region was governed by a southwestward subduction of the passive margin of the Tuva-Mongolian continental block during the Neoproterozoic to Early Cambrian. This resulted in the obduction of high-pressure rocks and ophiolitic fragments onto the continental basement at ~540Ma [*Štípská et al., 2010*] and the formation of an Early Cambrian accretionary system, i.e., the Lake Zone [*Kröner et al., 2010; Lehmann et al., 2010*]. A new NE dipping subduction probably

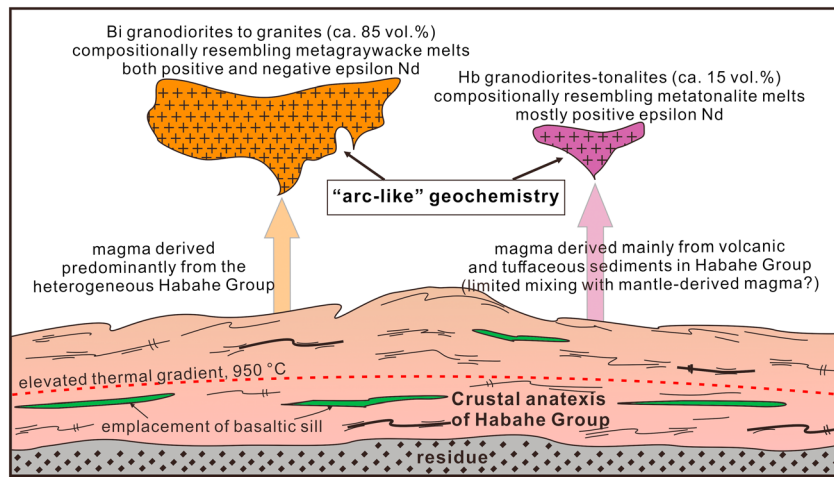


Figure 12. A tentative model for the formation of the granitoids in the Chinese Altai. Felsic melts are generated at depth via predominantly anatexitic reworking of the Habahe Group metasediments. Intermediate, hornblende-bearing granodiorites to tonalites are a result of partial melting of the volcanogenic components therein. Involvement of mantle-derived basaltic melts is possible but less significant than in previous interpretations [e.g., Wang *et al.*, 2009].

started since Early Cambrian and affected the SW margin of the Tuva-Mongolian block by widespread arc magmatism culminating at 500Ma [Janoušek *et al.*, 2014; Soejono *et al.*, 2016]. Continuous retreat of the subducting plate resulted in the formation of a huge turbidite fan, which received the erosion products from preexisting Late Proterozoic Lake Zone, Cambrian volcanic arcs, as well as Proterozoic basement rocks of the Tuva-Mongolian block. This giant sedimentary fan, together with accreted and imbricated ocean floor sediments and mafic volcanic rocks, constituted an Early Paleozoic accretionary wedge in the Hovd-Altai area [Xiao *et al.*, 2009].

As the youngest unit in the northern Mongolian CAO, the southern Altai has been assigned as an active margin in the Early-Middle Paleozoic [e.g., Xiao *et al.*, 2009; Long *et al.*, 2010]. The appearance of compositionally heterogeneous mafic rocks and the association of Silurian to Middle Devonian adakite+high-Mg andesite+boninite+Nb-enriched basalt were considered as proxies of an abrupt change in thermal regime along the active margin due to upwelling of hot asthenospheric mantle [e.g., Niu *et al.*, 2006; Cai *et al.*, 2010; Wong *et al.*, 2010]. In order to explain anomalous thermal conditions of the Chinese Altai in the Devonian, subduction of an active spreading oceanic ridge and associated asthenosphere upwelling were proposed [e.g., Sun *et al.*, 2009; Cai *et al.*, 2010; Jiang *et al.*, 2010]. Alternatively, the elevation of asthenosphere can be attributed to back-arc spreading or large-scale lithosphere thinning above the Pacific-type subduction systems [e.g., Collins, 2002; Currie *et al.*, 2004; Hyndman *et al.*, 2005]. Collins and Richards [2008] proposed that such a tectonic process would result in a focused heat advection responsible for massive melting of overriding fertile sedimentary back-arc sequences producing circum-Pacific S-type granitoids. In Cascadia, rather constant surface heat flow (Q_s) of 80–100mW/m² was reported in 400km wide region across the back arc of the central Andean extensional suprasubduction zone, suggesting extremely hot mantle flow [Currie *et al.*, 2004]. For such heat flow values, the temperatures at 30km can attain 770°C–1100°C, matching well with the proposed thermal conditions for the crustal anatexis in the Chinese Altai (Figure 4). It should be stressed that analogous large-scale extensional event associated with extensive Devonian partial melting of metasediments and emplacement of various amounts of gabbroic sheets was recently reported from the adjacent Mongolian Altai [Hanžl *et al.*, 2016]. Altogether, Silurian to Devonian granitoids in the Chinese Altai were probably produced during the same crustal extensional event associated with the upwelling of the asthenospheric mantle (Figure 13).

Although Collins [2002] and Collins and Richards [2008] envisaged remelting of previously thickened back arcs during lithospheric suprasubduction extension, the melting of thick accretionary system is equally possible, if not more likely, candidate to produce large quantities of granitoids. Pacific sedimentary prisms are several hundred kilometers wide and thousands of kilometers long structures [e.g., Şengör and Natal'in, 1996; Kusky *et al.*, 2013]. These wedge-like structures are composed of imbricated ocean plate stratigraphy

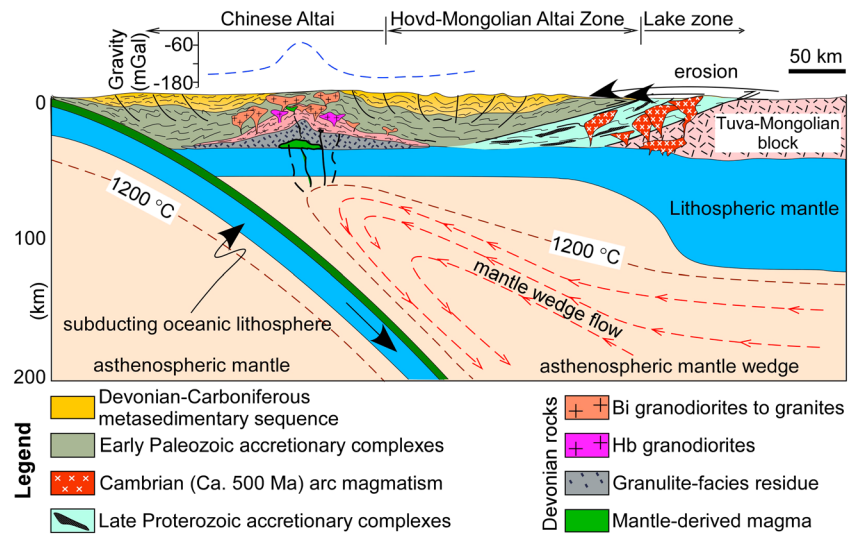


Figure 13. Tectonic interpretation for the generation of voluminous Silurian-Devonian granitoids and the formation of differentiated crust in the Chinese Altai due to lithosphere thinning and asthenosphere upwelling (modified after Collins [2002] and Hyndman et al. [2005]). Idealized gravity profile on the Chinese Altai and Hovd-Mongolian Altai regions shows nature of gravity anomalies related to deep structure of partially molten wedge.

sediments, basalts, and trench turbidites scrapped off from the subducting plate. The dominant component is the greywacke-type sediments with chemistry resembling to magmatic arcs [Lisitzin, 1972]. Retreat of the subduction zone is associated with trenchward migration of magmatic arcs and massive extension of the upper plate including accretionary wedges and is commonly related with intrusion of abundant arc-type granitoids [Şengör et al., 1993; Şengör and Natal'in, 1996]. Anatectic reworking of wedge sediments has been found to be an important process governing the magmatic evolution of the accretionary orogens, particularly in the circum-Pacific accretionary system [e.g., Barker et al., 1992; Shinjoe, 1997].

Modern geophysical studies of accretionary orogens show that individual accreted terranes commonly preserve a specific and strong geophysical signal (Bouguer and magnetic anomalies) distinctive for their origin and geological history [Glen et al., 2007; Burton, 2010]. However, this is not the case of the Altai accretionary wedge that features horizontally heterogeneous geophysical signal marked by high-density lower crust in the south (Chinese Altai) and low-density lower crust to the north (Mongolian Altai, Figures 10a and 10b). It can be theoretically assumed that the homogeneous gravity signal of the accretionary wedge was modified by localized tectonic or magmatic process. Here it is proposed that partial melting of the fertile Habahe Group metasediments is responsible for the origin of arc-like granitoids and heavy granulitic residue with density of 2890 kg/m^3 in the deep crust. As a consequence, it can account for the low-frequency gravity high in the Chinese Altai and the laterally heterogeneous gravity pattern across the Altai Orogen. In such a model, extraction and ascent of felsic melt to middle and upper crustal levels leave behind a dense and refractory lower crustal residue, leading to a large-scale differentiation of the crust. As such, it seems to represent a fundamental mechanism transforming accretionary wedges into vertically differentiated and stratified continental crust along Pacific-type continental margins.

6. Conclusions

Geological and geochemical data, thermodynamic modeling, and gravity analysis are combined to characterize the Silurian-Devonian magmatism and crustal evolution of the Chinese Altai Orogenic Belt. The principal conclusions are as follows:

1. Partial melting of the young, geochemically primitive Habahe Group metasediments may be considered as a viable source for the most (>85%) Silurian-Devonian granitoids in the Chinese Altai. The minor (<15%) hornblende tonalities to granodiorites could come from the volcanogenic components of the same unit or may be derived from the mantle. This model contrasts with previously proposed derivation of the granitoids with significant contribution (>50%) from juvenile mantle-derived melts.

2. Melting of the accretionary wedge could have led to formation of a heavy granulite residue, explaining the gravity high over the Chinese Altai.
3. Massive magmatism due to anatectic reworking of the accretionary wedge can result in the formation of differentiated and vertically stratified continental crust. Such a process may provide a key to the understanding of transformation of accretionary wedges into stabilized continents and the peripheral growth of continental crust in accretionary orogens.

Acknowledgments

This study was supported by the Strategic Priority Research Program (B) of the Chinese Academy of Sciences (XDB18020203), NSF China (41672056, 41190075, and 41273048), International Partnership Program of Chinese Academy of Sciences (132744KYSB20160005), and HKRGC grants (HKU705311P and HKU704712P). Postdoctoral fellowship from Charles University, 100 Talents Program of the Chinese Academy of Sciences, and a "Senior visiting fellowship" from the China Scholarship Council to Y.D. JIANG is acknowledged. This work is a contribution to IGCP 592 project "Continental construction in Central Asia." We also acknowledge the Czech Science Foundation (P210/12/2205) and the Ministry of Education of the Czech Republic (LK11202). Roberto Weinberg is thanked for his valuable comments on an earlier version of this manuscript. Comments from Journal reviewers Bill Collins and Stefan Jung and anonymous reviewer and editorial suggestions from Lothar Ratschbacher helped us to greatly improve the paper and are most appreciated. The data used are listed in the references and supporting information.

References

- Aguilar, C., M. Liesa, P. Štípská, K. Schulmann, J. A. Muñoz, and J. M. Casas (2015), *P–T–t* evolution of orogenic middle crust of the Roc de Frausa Massif (Eastern Pyrenees): A result of horizontal crustal flow and Carboniferous doming?, *J. Metamorph. Geol.*, *33*(3), 273–294, doi:10.1111/jmg.12120.
- Anderson, A. T. (1982), Parental basalts in subduction zones: Implications for continental evolution, *J. Geophys. Res.*, *87*, 7047–7060, doi:10.1029/JB087iB08p07047.
- Arculus, R. J. (2003), Use and abuse of the terms calcalkaline and calcalkalic, *J. Petrol.*, *44*(5), 929–935, doi:10.1093/ptrology/44.5.929.
- Artemieva, I. M., and R. Meissner (2012), Crustal thickness controlled by plate tectonics: A review of crust–mantle interaction processes illustrated by European examples, *Tectonophysics*, *530–531*, 18–49, doi:10.1016/j.tecto.2011.12.037.
- Auzanneau, E., M. W. Schmidt, D. Vielzeuf, and J. A. D. Connolly (2010), Titanium in phengite: A geobarometer for high temperature eclogites, *Contrib. Mineral. Petrol.*, *159*(1), 1–24, doi:10.1007/s00410-009-0412-7.
- Badarch, G., W. Dickson Cunningham, and B. F. Windley (2002), A new terrane subdivision for Mongolia: Implications for the Phanerozoic crustal growth of Central Asia, *J. Asian Earth Sci.*, *21*(1), 87–110, doi:10.1016/S1367-9120(02)00017-2.
- Baker, P. E. (1968), Comparative volcanology and petrology of the Atlantic island-arcs, *Bull. Volcanol.*, *32*(1), 189–206, doi:10.1007/bf02596591.
- Balmino, G., N. Vales, S. Bonvalot, and A. Briais (2012), Spherical harmonic modeling to ultra-high degree of Bouguer and isostatic anomalies, *J. Geod.*, *86*(7), 499–520, doi:10.1007/s00190-011-0533-4.
- Barker, F., G. L. Farmer, R. A. Ayuso, G. Plafker, and J. S. Lull (1992), The 50Ma granodiorite of the eastern Gulf of Alaska: Melting in an accretionary prism in the forearc, *J. Geophys. Res.*, *97*, 6757–6778, doi:10.1029/92JB00257.
- Barry, T. L., A. D. Saunders, P. D. Kempton, B. F. Windley, M. S. Pringle, D. Dorjnamjaa, and S. Saandar (2003), Petrogenesis of Cenozoic basalts from Mongolia: Evidence for the role of asthenospheric versus metasomatized lithospheric mantle sources, *J. Petrol.*, *44*(1), 55–91, doi:10.1093/ptrology/44.1.55.
- Bhatia, M. R., and K. A. W. Crook (1986), Trace element characteristics of graywackes and tectonic setting discrimination of sedimentary basins, *Contrib. Mineral. Petrol.*, *92*(2), 181–193, doi:10.1007/bf00375292.
- Bian, W., J. Hornung, Z. Liu, P. Wang, and M. Hinderer (2010), Sedimentary and palaeoenvironmental evolution of the Junggar Basin, Xinjiang, Northwest China, *Palaeobiodiversity Palaeoenviron.*, *90*(3), 175–186, doi:10.1007/s12549-010-0038-9.
- Bickle, M. J., S. M. Wickham, H. J. Chapman, and H. P. Taylor (1988), A strontium, neodymium and oxygen isotope study of hydrothermal metamorphism and crustal anatexis in the Trois Seigneurs Massif, Pyrenees, France, *Contrib. Mineral. Petrol.*, *100*(4), 399–417, doi:10.1007/bf00371371.
- Borg, L. E., and M. A. Clyne (1998), The petrogenesis of felsic calc-alkaline magmas from the southernmost Cascades, California: Origin by partial melting of basaltic lower crust, *J. Petrol.*, *39*(6), 1197–1222, doi:10.1093/ptrology/39.6.1197.
- Brousolle, A., et al. (2015), *P–T–t* record of crustal-scale horizontal flow and magma-assisted doming in the SW Mongolian Altai, *J. Metamorph. Geol.*, *33*(4), 359–383, doi:10.1111/jmg.12124.
- Brown, M. (2010), Melting of the continental crust during orogenesis: The thermal, rheological, and compositional consequences of melt transport from lower to upper continental crust, *Can. J. Earth Sci.*, *47*(5), 655–694, doi:10.1139/E09-057.
- Burenjargal, U., A. Okamoto, T. Kuwatani, S. Sakata, T. Hirata, and N. Tsuchiya (2014), Thermal evolution of the Tseel terrane, SW Mongolia and its relation to granitoid intrusions in the Central Asian Orogenic Belt, *J. Metamorph. Geol.*, *32*(7), 765–790, doi:10.1111/jmg.12090.
- Burton, G. R. (2010), New structural model to explain geophysical features in northwestern New South Wales: Implications for the tectonic framework of the Tasmanides, *Aust. J. Earth Sci.*, *57*(1), 23–49, doi:10.1080/08120090903416195.
- Cai, K., M. Sun, C. Yuan, G. Zhao, W. Xiao, X. Long, and F. Wu (2010), Geochronological and geochemical study of mafic dykes from the northwest Chinese Altai: Implications for petrogenesis and tectonic evolution, *Gondwana Res.*, *18*(4), 638–652, doi:10.1016/j.gr.2010.02.010.
- Cai, K., M. Sun, C. Yuan, X. Long, and W. Xiao (2011a), Geological framework and Paleozoic tectonic history of the Chinese Altai, NW China: A review, *Russ. Geol. Geophys.*, *52*(12), 1619–1633, doi:10.1016/j.rgg.2011.11.014.
- Cai, K., M. Sun, C. Yuan, G. Zhao, W. Xiao, X. Long, and F. Wu (2011b), Geochronology, petrogenesis and tectonic significance of peraluminous granites from the Chinese Altai, NW China, *Lithos*, *127*(1–2), 261–281, doi:10.1016/j.lithos.2011.09.001.
- Cai, K., M. Sun, C. Yuan, G. Zhao, W. Xiao, and X. Long (2012), Keketuohai mafic–ultramafic complex in the Chinese Altai, NW China: Petrogenesis and geodynamic significance, *Chem. Geol.*, *294–295*, 26–41, doi:10.1016/j.chemgeo.2011.11.031.
- Cawood, P. A., A. Kröner, W. J. Collins, T. M. Kusky, W. D. Mooney, and B. F. Windley (2009), Accretionary orogens through Earth history, in *Earth Accretionary Systems in Space and Time*, vol. 318(1), edited by P. A. Cawood and A. Kröner, pp. 1–36, Geol. Soc. London Spec. Publ., doi:10.1144/sp318.1.
- Chai, F., J. Mao, L. Dong, F. Yang, F. Liu, X. Geng, and Z. Zhang (2009), Geochronology of metarhyolites from the Kangbutiebao Formation in the Kelang basin, Altay Mountains, Xinjiang: Implications for the tectonic evolution and metallogeny, *Gondwana Res.*, *16*(2), 189–200, doi:10.1016/j.gr.2009.03.002.
- Chai, F., L. Dong, F. Yang, F. Liu, X. Geng, and C. Huang (2010), Age, geochemistry and petrogenesis of the Tiemierte granites in the Kelang basin at the southern margin of Altay, Xinjiang, *Acta Geol. Sin.*, *26*, 377–386.
- Chen, B., and B. M. Jahn (2002), Geochemical and isotopic studies of the sedimentary and granitic rocks of the Altai orogen of northwest China and their tectonic implications, *Geol. Mag.*, *139*(01), 1–13, doi:10.1017/S0016756801006100.
- Clemens, J. D., and G. Stevens (2012), What controls chemical variation in granitic magmas?, *Lithos*, *134–135*, 317–329, doi:10.1016/j.lithos.2012.01.001.
- Coggon, R., and T. J. B. Holland (2002), Mixing properties of phengitic micas and revised garnet–phengite thermobarometers, *J. Metamorph. Geol.*, *20*(7), 683–696, doi:10.1046/j.1525-1314.2002.00395.x.

- Collins, W. J. (2002), Hot orogens, tectonic switching, and creation of continental crust, *Geology*, *30*(6), 535–538, doi:10.1130/0091-7613(2002)030<0535:hotsac>2.0.co;2.
- Collins, W. J., and S. W. Richards (2008), Geodynamic significance of S-type granites in circum-Pacific orogens, *Geology*, *36*(7), 559–562, doi:10.1130/g24658a.1.
- Connolly, J. A. D. (2005), Computation of phase equilibria by linear programming: A tool for geodynamic modeling and its application to subduction zone decarbonation, *Earth Planet. Sci. Lett.*, *236*(1–2), 524–541, doi:10.1016/j.epsl.2005.04.033.
- Conrad, W. K., I. A. Nicholle, and V. J. Wall (1988), Water-saturated and -undersaturated melting of metaluminous and peraluminous crustal compositions at 10 kb: Evidence for the origin of silicic magmas in the taupo volcanic zone, New Zealand, and other occurrences, *J. Petrol.*, *29*(4), 765–803, doi:10.1093/petrology/29.4.765.
- Currie, C. A., K. Wang, R. D. Hyndman, and J. He (2004), The thermal effects of steady-state slab-driven mantle flow above a subducting plate: The Cascadia subduction zone and backarc, *Earth Planet. Sci. Lett.*, *223*(1–2), 35–48, doi:10.1016/j.epsl.2004.04.020.
- Debon, F., and P. Le Fort (1983), A chemical–mineralogical classification of common plutonic rocks and associations, *Earth Environ. Sci. Trans. R. Soc. Edinburgh*, *73*(03), 135–149, doi:10.1017/S0263593300010117.
- De la Roche, H., J. Leterrier, P. Grandclaude, and M. Marchal (1980), A classification of volcanic and plutonic rocks using R_1R_2 -diagram and major-element analyses—Its relationships with current nomenclature, *Chem. Geol.*, *29*(1–4), 183–210, doi:10.1016/0009-2541(80)90020-0.
- Diener, J. F. A., R. Powell, R. W. White, and T. J. B. Holland (2007), A new thermodynamic model for clino- and orthoamphiboles in the system $\text{Na}_2\text{O}-\text{CaO}-\text{FeO}-\text{MgO}-\text{Al}_2\text{O}_3-\text{SiO}_2-\text{H}_2\text{O}-\text{O}$, *J. Metamorph. Geol.*, *25*(6), 631–656, doi:10.1111/j.1525-1314.2007.00720.x.
- Downes, H. (1993), The nature of the lower continental crust of Europe: Petrological and geochemical evidence from xenoliths, *Phys. Earth Planet. Inter.*, *79*(1), 195–218, doi:10.1016/0031-9201(93)90148-3.
- Druguet, E. (2001), Development of high thermal gradients by coeval transpression and magmatism during the Variscan orogeny: Insights from the Cap de Creus (Eastern Pyrenees), *Tectonophysics*, *332*(1–2), 275–293, doi:10.1016/S0040-1951(00)00261-4.
- Ducea, M. N., S. Kidder, and G. Zandt (2003), Arc composition at mid-crustal depths: Insights from the Coast Ridge Belt, Santa Lucia Mountains, California, *Geophys. Res. Lett.*, *30*(13), 1703, doi:10.1029/2002GL016297.
- Ebadi, A., and W. Johannes (1991), Beginning of melting and composition of first melts in the system $\text{Qz}-\text{Ab}-\text{Or}-\text{H}_2\text{O}-\text{CO}_2$, *Contrib. Mineral. Petrol.*, *106*(3), 286–295, doi:10.1007/bf00324558.
- Floyd, P. A., and B. E. Leveridge (1987), Tectonic environment of the Devonian Gramscatho basin, south Cornwall: Framework mode and geochemical evidence from turbiditic sandstones, *J. Geol. Soc.*, *144*(4), 531–542, doi:10.1144/gsjgs.144.4.0531.
- Gerdes, A., P. Montero, F. Bea, G. Fershter, N. Borodina, T. Osipova, and G. Shardakova (2002), Peraluminous granites frequently with mantle-like isotope compositions: The continental-type Murzinka and Dzhabyk batholiths of the eastern Urals, *Int. J. Earth Sci.*, *91*(1), 3–19, doi:10.1007/s005310100195.
- Glen, J. M. G., J. Schmidt, and R. Morin (2007), Gravity and magnetic character of south-central Alaska: Constraints on geologic and tectonic interpretations, and implications for mineral exploration, *Geol. Soc. Am. Spec. Pap.*, *431*, 593–622, doi:10.1130/2007.2431(23).
- Green, E., T. Holland, and R. Powell (2007), An order-disorder model for omphacitic pyroxenes in the system jadeite–diopside–hedenbergite–acmite, with applications to eclogitic rocks, *Am. Mineral.*, *92*(7), 1181–1189, doi:10.2138/am.2007.2401.
- Green, E. C. R., R. W. White, J. F. A. Diener, R. Powell, T. J. B. Holland, and R. M. Palin (2016), Activity–composition relations for the calculation of partial melting equilibria in metabasic rocks, *J. Metamorph. Geol.*, doi:10.1111/jmg.12211, in press.
- Guy, A., et al. (2015), Geophysical and geochemical nature of re-laminated arc-derived lower crust underneath oceanic domain in southern Mongolia, *Tectonics*, *34*(5), 1030–1053, doi:10.1002/2015TC003845.
- Hanžl, P., K. Schulmann, V. Janoušek, O. Lexa, K. Hrdličková, Y. Jiang, D. Buriánek, B. Altanbaatar, T. Ganchuluun, and V. Erban (2016), Making continental crust: Origin of Devonian orthogneisses from SE Mongolian Altai, *J. Geosci.*, *61*(1), 25–50, doi:10.3190/jgeosci.206.
- Harris, N. B. W., and S. Inger (1992), Trace element modelling of pelite-derived granites, *Contrib. Mineral. Petrol.*, *110*(1), 46–56, doi:10.1007/bf00310881.
- Hartel, T. H. D., and D. R. M. Pattison (1996), Genesis of the Kapuskasing (Ontario) migmatitic mafic granulites by dehydration melting of amphibolite: The importance of quartz to reaction progress, *J. Metamorph. Geol.*, *14*(5), 591–611, doi:10.1046/j.1525-1314.1996.00404.x.
- Heiskanen, W. A., and H. Moritz (1967), *Physical Geodesy*, 364 pp., W.H. Freeman, San Francisco, Calif.
- Hinze, W. J., R. R. B. Von Frese, and A. H. Saad (2013), *Gravity and Magnetic Exploration: Principle, Practices and Applications*, 502 pp., Cambridge Univ. Press, Cambridge, U. K.
- Holbrook, W. S., D. Lizarralde, S. McGeary, N. Bangs, and J. Diebold (1999), Structure and composition of the Aleutian island arc and implications for continental crustal growth, *Geology*, *27*(1), 31–34, doi:10.1130/0091-7613(1999)027<0031:sacota>2.3.co;2.
- Holland, T., and R. Powell (2003), Activity–composition relations for phases in petrological calculations: An asymmetric multicomponent formulation, *Contrib. Mineral. Petrol.*, *145*(4), 492–501, doi:10.1007/s00410-003-0464-z.
- Holland, T., J. Baker, and R. Powell (1998), Mixing properties and activity–composition and relationships of chlorites in the system $\text{MgO}-\text{FeO}-\text{Al}_2\text{O}_3-\text{SiO}_2-\text{H}_2\text{O}$, *Eur. J. Mineral.*, *10*(3), 395–406, doi:10.1127/ejm/10/3/0395.
- Holland, T. J. B., and R. Powell (1998), An internally consistent thermodynamic data set for phases of petrological interest, *J. Metamorph. Geol.*, *16*(3), 309–343, doi:10.1111/j.1525-1314.1998.00140.x.
- Hu, A., B. M. Jahn, G. Zhang, Y. Chen, and Q. Zhang (2000), Crustal evolution and Phanerozoic crustal growth in northern Xinjiang: Nd isotopic evidence—Part I. Isotopic characterization of basement rocks, *Tectonophysics*, *328*(1–2), 15–51, doi:10.1016/S0040-1951(00)00176-1.
- Hyndman, R. D., C. A. Currie, and S. Mazzotti (2005), Subduction zone backarcs, continental mobile belts, and orogenic heat, *GSA Today*, *15*, 4–10, doi:10.1130/1052-5173(2005)015:e8:SZBMB.2.0.co;2.
- Jacobsen, S. B., and G. J. Wasserburg (1980), Sm–Nd isotopic evolution of chondrites, *Earth Planet. Sci. Lett.*, *50*(1), 139–155, doi:10.1016/0012-821X(80)90125-9.
- Jagoutz, O., and M. W. Schmidt (2012), The formation and bulk composition of modern juvenile continental crust: The Kohistan arc, *Chem. Geol.*, *298*–299, 79–96, doi:10.1016/j.chemgeo.2011.10.022.
- Jahn, B. M., and K. C. Condie (1995), Evolution of the Kaapvaal–Craton as viewed from geochemical and Sm–Nd isotopic analyses of intracratonic pelites, *Geochim. Cosmochim. Acta*, *59*, 2239–2258, doi:10.1016/0016-7037(95)00103-7.
- Jahn, B. M., F. Y. Wu, and B. Chen (2000), Granitoids of the Central Asian Orogenic Belt and continental growth in the Phanerozoic, *Trans. R. Soc. Edinburgh: Earth Sci.*, *91*, 181–193, doi:10.1017/S0263593300007367.
- Jahn, B. M., B. Windley, B. Natal'in, and N. Dobretsov (2004), Phanerozoic continental growth in Central Asia, *J. Asian Earth Sci.*, *23*(5), 599–603, doi:10.1016/S1367-9120(03)00124-X.
- Janoušek, V., C. M. Farrow, and V. Erban (2006), Interpretation of whole-rock geochemical data in igneous geochemistry: Introducing Geochemical Data Toolkit (GCDkit), *J. Petrol.*, *47*(6), 1255–1259, doi:10.1093/petrology/egl013.

- Janoušek, V., J. Konopásek, S. Ulrich, V. Erban, L. Tajčmanová, and P. Jeřábek (2010), Geochemical character and petrogenesis of Pan-African Amspoort suite of the Boundary Igneous Complex in the Kaoko Belt (NW Namibia), *Gondwana Res.*, *18*(4), 688–707, doi:10.1016/j.jgr.2010.02.014.
- Janoušek, V., Y. Jiang, K. Schulmann, D. Burianek, P. Hanžl, O. Lexa, T. Gunchuluun, and A. Battushig (2014), The age, nature and likely genesis of the Cambrian Khantaishir arc, Lake Zone, Mongolia, paper presented at EGU General Assembly 2014, Vienna.
- Janoušek, V., J. F. Moya, H. Martin, V. Erban, and C. Farrow (2016), *Geochemical Modelling of Igneous Processes—Principles and Recipes in R Language*, Springer, Berlin, doi:10.1007/978-3-662-46792-3.
- Jiang, Y., M. Sun, G. Zhao, C. Yuan, W. Xiao, X. Xia, X. Long, and F. Wu (2010), The ~390 Ma high-T metamorphic event in the Chinese Altai: A consequence of ridge-subduction?, *Am. J. Sci.*, *310*(10), 1421–1452, doi:10.2475/10.2010.08.
- Jiang, Y., M. Sun, G. Zhao, C. Yuan, W. Xiao, X. Xia, X. Long, and F. Wu (2011), Precambrian detrital zircons in the Early Paleozoic Chinese Altai: Their provenance and implications for the crustal growth of central Asia, *Precambrian Res.*, *189*(1–2), 140–154, doi:10.1016/j.precamres.2011.05.008.
- Jiang, Y., M. Sun, A. Kröner, D. Tumurkhuu, X. Long, G. Zhao, C. Yuan, and W. Xiao (2012), The high-grade Tseel Terrane in SW Mongolia: An Early Paleozoic arc system or a Precambrian sliver?, *Lithos*, *142*, 95–115, doi:10.1016/j.lithos.2012.02.016.
- Jiang, Y. D., et al. (2015), Juxtaposition of Barrovian and migmatite domains in the Chinese Altai: A result of crustal thickening followed by doming of partially molten lower crust, *J. Metamorph. Geol.*, *33*(1), 45–70, doi:10.1111/jmg.12110.
- Kilzi, M. A., M. Grégoire, V. Bosse, M. Benoit, Y. Driouch, M. de Saint Blanquat, and P. Debat (2016), Geochemistry and zircon U–Pb geochronology of the ultramafic and mafic rocks emplaced within the anatectic series of the Variscan Pyrenees: The example of the Gavarnie–Heas dome (France), *C. R. Geosci.*, *348*(2), 107–115, doi:10.1016/j.crte.2015.06.014.
- Kovach, V. P., V. V. Yarmolyuk, V. I. Kovalenko, A. M. Kozlovskiy, A. B. Kotov, and L. B. Terent'eva (2011), Composition, sources, and mechanisms of formation of the continental crust of the Lake zone of the Central Asian Caledonides: II. Geochemical and Nd isotope data, *Petrology*, *19*(4), 399–425, doi:10.1134/S0869591111030064.
- Kovalenko, V. I., V. V. Yarmolyuk, V. P. Kovach, A. B. Kotov, I. K. Kozakov, E. B. Salnikova, and A. M. Larin (2004), Isotope provinces, mechanisms of generation and sources of the continental crust in the Central Asian mobile belt: Geological and isotopic evidence, *J. Asian Earth Sci.*, *23*(5), 605–627, doi:10.1016/S1367-9120(03)00130-5.
- Kozakov, I., V. A. Glebovitsky, E. V. Bibikova, P. Y. Azimov, and T. I. Kirnozova (2002), Hercynian granulites of Mongolian and Gobian Altai: Geodynamic setting and formation conditions, *Dokl. Earth Sci.*, *38*, 781–785.
- Kröner, A., J. Lehmann, K. Schulmann, A. Demoux, O. Lexa, D. Tomurhuu, P. Štípská, D. Liu, and M. T. D. Wingate (2010), Lithostratigraphic and geochronological constraints on the evolution of the Central Asian Orogenic Belt in SW Mongolia: Early Paleozoic rifting followed by Late Paleozoic accretion, *Am. J. Sci.*, *310*(7), 523–574, doi:10.2475/07.2010.01.
- Kröner, A., et al. (2014), Reassessment of continental growth during the accretionary history of the Central Asian Orogenic Belt, *Gondwana Res.*, *25*(1), 103–125, doi:10.1016/j.jgr.2012.12.023.
- Kusky, T. M., B. F. Windley, I. Safonova, K. Wakita, J. Wakabayashi, A. Polat, and M. Santosh (2013), Recognition of ocean plate stratigraphy in accretionary orogens through Earth history: A record of 3.8 billion years of sea floor spreading, subduction, and accretion, *Gondwana Res.*, *24*(2), 501–547, doi:10.1016/j.jgr.2013.01.004.
- Laske, G., Z. G. Masters, and M. Pasyanos (2013), Update on CRUST1.0-A1-degree global model of Earth's crust, *Geophys. Res. Abstr.*, *15*, Abstract EGU2013-2658.
- Lehmann, J., K. Schulmann, O. Lexa, M. Corsini, A. Kröner, P. Štípská, D. Tomurhuu, and D. Otgonbator (2010), Structural constraints on the evolution of the Central Asian Orogenic Belt in SW Mongolia, *Am. J. Sci.*, *310*(7), 575–628, doi:10.2475/07.2010.02.
- Li, H. Q., C. Xie, H. Chang, H. Cai, J. P. Zhu, and S. Zhou (Eds) (1998), *Study on Metallogenetic Chronology of Nonferrous and Precious Metallic Ore Deposits in North Xinjiang, China*, 171 pp., Geol. House, Beijing.
- Li, X. H., Z. X. Li, H. Zhou, Y. Liu, and P. D. Kinny (2002), U–Pb zircon geochronology, geochemistry and Nd isotopic study of Neoproterozoic bimodal volcanic rocks in the Kangdian Rift of South China: Implications for the initial rifting of Rodinia, *Precambrian Res.*, *113*(1–2), 135–154, doi:10.1016/S0301-9268(01)00207-8.
- Li, X. H., D. Y. Liu, M. Sun, W. X. Li, X. R. Liang, and Y. Liu (2004), Precise Sm–Nd and U–Pb isotopic dating of the supergiant Shizhuyuan polymetallic deposit and its host granite, SE China, *Geol. Mag.*, *141*(2), 225–231, doi:10.1017/s0016756803008823.
- Li, Z., Y. Li, H. Chen, M. Santosh, W. Xiao, and H. Wang (2010), SHRIMP U–Pb zircon chronology of ultrahigh-temperature spinel-orthopyroxene-garnet granulite from South Altay orogenic belt, northwestern China, *Isl. Arc*, *19*(3), 506–516, doi:10.1111/j.1440-1738.2010.00726.x.
- Li, Z. L., X. Q. Yang, Y. Q. Li, M. Santosh, H. L. Chen, and W. J. Xiao (2014), Late Paleozoic tectono-metamorphic evolution of the Altai segment of the Central Asian Orogenic Belt: Constraints from metamorphic P–T pseudosection and zircon U–Pb dating of ultra-high-temperature granulite, *Lithos*, *204*, 83–96, doi:10.1016/j.lithos.2014.05.022.
- Lisitzin, A. P. (1972), *Sedimentation in the World Ocean, Spec. Publ.*, vol. 17, 218 pp., Soc. of Econ. Paleontol. and Mineral, Tulsa, Okla.
- Liu, W., X. J. Liu, and W. J. Xiao (2012), Massive granitoid production without massive continental-crust growth in the Chinese Altai: Insight into the source rock of granitoids using integrated zircon U–Pb age, Hf–Nd–Sr isotopes and geochemistry, *Am. J. Sci.*, *312*(6), 629–684, doi:10.2475/06.2012.02.
- Long, X., M. Sun, C. Yuan, W. Xiao, and K. Cai (2008), Early Paleozoic sedimentary record of the Chinese Altai: Implications for its tectonic evolution, *Sediment. Geol.*, *208*(3–4), 88–100, doi:10.1016/j.sedgeo.2008.05.002.
- Long, X., C. Yuan, M. Sun, W. Xiao, G. Zhao, Y. Wang, K. Cai, X. Xia, and L. Xie (2010), Detrital zircon ages and Hf isotopes of the early Paleozoic Habahe sequence in the Chinese Altai, NW China: New constraints on depositional age, provenance and tectonic evolution, *Tectonophysics*, *480*, 213–231, doi:10.1016/j.tecto.2009.10.013.
- Long, X., C. Yuan, M. Sun, W. Xiao, Y. Wang, K. Cai, and Y. Jiang (2012), Geochemistry and Nd isotopic composition of the Early Paleozoic Habahe sequence in the Chinese Altai, Central Asia: Evidence for a northward-derived mafic source and insight into Nd model ages in accretionary orogen, *Gondwana Res.*, *22*(2), 554–566, doi:10.1016/j.jgr.2011.04.009.
- Miller, R. G., and R. K. O'Nions (1985), Source of Precambrian chemical and clastic sediments, *Nature*, *314*, 325–330, doi:10.1038/314325a0.
- Montel, J. M., and D. Vielzeuf (1997), Partial melting of metagreywackes: Part II. Compositions of minerals and melts, *Contrib. Mineral. Petrol.*, *128*(2–3), 176–196, doi:10.1007/s004100050302.
- Nakano, N., Y. Osanai, M. Owada, M. Satish-Kumar, T. Adachi, S. Jargalan, A. Yoshimoto, K. Syeryekhan, and C. Boldbaatar (2015), Multiple growth of garnet, sillimanite/kyanite and monazite during amphibolite facies metamorphism: Implications for the P–T–t and tectonic evolution of the western Altai Range, Mongolia, *J. Metamorph. Geol.*, *33*(9), 937–958, doi:10.1111/jmg.12154.
- Niu, H., H. Sato, H. Zhang, J. I. Ito, X. Yu, T. Nagao, K. Terada, and Q. Zhang (2006), Juxtaposition of adakite, boninite, high-TiO₂ and low-TiO₂ basalts in the Devonian southern Altay, Xinjiang, NW China, *J. Asian Earth Sci.*, *28*(4–6), 439–456, doi:10.1016/j.jseas.2005.11.010.

- Othman, D. B., S. Fourcade, and C. J. Allègre (1984), Recycling processes in granite-granodiorite complex genesis: The Querigut case studied by Nd-Sr isotope systematics, *Earth Planet. Sci. Lett.*, *69*(2), 290–300, doi:10.1016/0012-821X(84)90188-2.
- Patiño Douce, A. E., and J. S. Beard (1995), Dehydration-melting of Biotite Gneiss and Quartz Amphibolite from 3 to 15 kbar, *J. Petrol.*, *36*(3), 707–738, doi:10.1093/ptrology/36.3.707.
- Pettijohn, F. J., P. E. Potter, and R. Siever (1987), *Sand and Sandstone*, 2nd ed., 553 pp., Springer, New York.
- Plank, T., and C. H. Langmuir (1998), The chemical composition of subducting sediment and its consequences for the crust and mantle, *Chem. Geol.*, *145*(3–4), 325–394, doi:10.1016/S0009-2541(97)00150-2.
- Powell, R., and T. Holland (1999), Relating formulations of the thermodynamics of mineral solid solutions; activity modeling of pyroxenes, amphiboles, and micas, *Am. Mineral.*, *84*(1–2), 1–14, doi:10.2138/am-1999-1-201.
- Rapp, R. P., and E. B. Watson (1995), Dehydration melting of metabasalt at 8–32 kbar: Implications for continental growth and crust-mantle recycling, *J. Petrol.*, *36*(4), 891–931, doi:10.1093/ptrology/36.4.891.
- Rey, P., J. P. Burg, and M. Casey (1997), The Scandinavian Caledonides and their relationship to the Variscan belt, in *Orogeny Through Time, Spec. Publ.*, vol. 121(1), edited by J.-P. Burg and M. Ford, pp. 179–200, Geol. Soc. London Spec. Publ., doi:10.1144/gsl.sp.1997.121.01.08.
- Ringwood, A. E. (1974), The petrological evolution of island arc systems: Twenty-seventh William Smith Lecture, *J. Geol. Soc.*, *130*(3), 183–204, doi:10.1144/gsjgs.130.3.0183.
- Roberts, M. P., C. Pin, J. D. Clemens, and J. L. Paquette (2000), Petrogenesis of mafic to felsic plutonic rock associations: The calc-alkaline Quérigut Complex, French Pyrenees, *J. Petrol.*, *41*(6), 809–844, doi:10.1093/ptrology/41.6.809.
- Rollinson, H. (2008), Secular evolution of the continental crust: Implications for crust evolution models, *Geochem. Geophys. Geosyst.*, *9*, Q12010, doi:10.1029/2008GC002262.
- Rossi, P., and A. Cocherie (1991), Genesis of a Variscan batholith: Field, petrological and mineralogical evidence from the Corsica-Sardinia batholith, *Tectonophysics*, *195*(2), 319–346, doi:10.1016/0040-1951(91)90219-1.
- Rudnick, R. L. (1995), Making continental crust, *Nature*, *378*(6557), 571–578, doi:10.1038/378571a0.
- Rudnick, R. L., and S. Gao (2003), Composition of the continental crust, in *The Crust, Treatise in Geochemistry*, vol. 3, edited by H. D. Holland and K. K. Turekian, pp. 1–64, Pergamon, Oxford.
- Şengör, A. M. C., and B. A. Natal'in (1996), Turcic-type orogeny and its role in the making of the continental crust, *Annu. Rev. Earth Planet. Sci.*, *24*(1), 263–337, doi:10.1146/annurev.earth.24.1.263.
- Şengör, A. M. C., B. A. Natal'in, and V. S. Burtman (1993), Evolution of the Altai tectonic collage and Paleozoic crustal growth in Eurasia, *Nature*, *364*, 299–307, doi:10.1038/364299a0.
- Shinjo, H. (1997), Origin of the granodiorite in the forearc region of southwest Japan: Melting of the Shimanto accretionary prism, *Chem. Geol.*, *134*(4), 237–255, doi:10.1016/S0009-2541(96)00062-9.
- Skjerlie, K. P., and A. E. Patiño Douce (1995), Anatectic interlayered amphibolite and pelite at 10 kbar: Effect of diffusion of major components on phase relations and melt fraction, *Contrib. Mineral. Petrol.*, *122*(1), 62–78, doi:10.1007/s004100050113.
- Soejono, I., D. Buriánek, M. Svojtka, V. Žáček, P. Čáp, and V. Janoušek (2016), Mid-Ordovician and Late Devonian magmatism in the Togtokhinshil Complex: New insight into the formation and accretionary evolution of the Lake Zone (western Mongolia), *J. Geosci.*, *61*(1), 5–23, doi:10.3190/jgeosci.208.
- Solano, J. M. S., M. D. Jackson, R. S. J. Sparks, J. D. Blundy, and C. Annen (2012), Melt segregation in deep crustal hot zones: A mechanism for chemical differentiation, crustal assimilation and the formation of evolved Magmas, *J. Petrol.*, *53*(10), 1999–2026, doi:10.1093/ptrology/egs041.
- Soula, J. C., P. Debat, J. Deramond, and P. Pouget (1986), A dynamic model of the structural evolution of the Hercynian Pyrenees, *Tectonophysics*, *129*(1), 29–51, doi:10.1016/0040-1951(86)90244-1.
- Štípská, P., K. Schulmann, J. Lehmann, M. Corsini, O. Lexa, and D. Tomurhuu (2010), Early Cambrian eclogites in SW Mongolia: Evidence that the Palaeo-Asian Ocean suture extends further east than expected, *J. Metamorph. Geol.*, *28*(9), 915–933, doi:10.1111/j.1525-1314.2010.00899.x.
- Sun, M., C. Yuan, W. Xiao, X. Long, X. Xia, G. Zhao, S. Lin, F. Wu, and A. Kröner (2008), Zircon U–Pb and Hf isotopic study of gneissic rocks from the Chinese Altai: Progressive accretionary history in the early to middle Palaeozoic, *Chem. Geol.*, *247*(3–4), 352–383, doi:10.1016/j.chemgeo.2007.10.026.
- Sun, M., X. Long, K. Cai, Y. Jiang, B. Wang, C. Yuan, G. Zhao, W. Xiao, and F. Wu (2009), Early Paleozoic ridge subduction in the Chinese Altai: Insight from the abrupt change in zircon Hf isotopic compositions, *Sci. China, Ser. D: Earth Sci.*, *52*(9), 1345–1358, doi:10.1007/s11430-009-0110-3.
- Sun, S. S., and W. F. McDonough (1989), Chemical and isotopic systematics of oceanic basalts: Implications for mantle composition and processes, in *Magmatism in the Ocean Basins*, vol. 42, edited by A. D. Sanders and M. J. Norry, pp. 313–345, Geol. Soc. London Spec. Publ., doi:10.1144/GSL.SP.1989.042.01.19.
- Sylvester, P. J. (1998), Post-collisional strongly peraluminous granites, *Lithos*, *45*(1–4), 29–44, doi:10.1016/S0024-4937(98)00024-3.
- Taylor, S. R. (1967), The origin and growth of continents, *Tectonophysics*, *4*(1), 17–34, doi:10.1016/0040-1951(67)90056-X.
- Taylor, S. R., and S. M. McLennan (1985), *The Continental Crust: Its Composition and Evolution*, 312 pp., Blackwell Sci., Oxford, U. K.
- Telford, W. M., L. P. Geldart, and R. E. Sheriff (1990), *Applied Geophysics*, 2nd ed., 860 pp., Cambridge Univ. Press, Cambridge, U. K.
- Thompson, A. B., K. Schulmann, J. Jezek, and V. Tolar (2001), Thermally softened continental extensional zones (arcs and rifts) as precursors to thickened orogenic belts, *Tectonophysics*, *332*(1–2), 115–141, doi:10.1016/S0040-1951(00)00252-3.
- Tong, Y., T. Wang, D. W. Hong, Y. J. Dai, B. F. Hang, and X. M. Liu (2007), Ages and origin of the early Devonian granites from the north part of Chinese Altai Mountains and its tectonic implications, *Acta Petrol. Sin.*, *23*(8), 1933–1944.
- Vilà, M., C. Pin, P. Enrique, and M. Liesa (2005), Telescoping of three distinct magmatic suites in an orogenic setting: Generation of Hercynian igneous rocks of the Albera Massif (Eastern Pyrenees), *Lithos*, *83*(1–2), 97–127, doi:10.1016/j.lithos.2005.01.002.
- Villaseca, C., L. Barbero, and V. Herreros (1998), A re-examination of the typology of peraluminous granite types in intracontinental orogenic belts, *Trans. R. Soc. Edinburgh: Earth Sci.*, *89*, 113–119, doi:10.1017/S0263593300007045.
- Waldbaum, D. R., and J. B. Thompson (1968), Mixing properties of sanidine crystalline solutions: II. Calculations based on volume data, *Am. Mineral.*, *53*, 2000–2017.
- Wang, T., D. W. Hong, B. M. Jahn, Y. Tong, Y. B. Wang, B. F. Hang, and X. X. Wang (2006), Timing, petrogenesis, and setting of Paleozoic synorogenic intrusions from the Altai Mountains, northwest China: Implications for the tectonic evolution of an accretionary orogen, *J. Geol.*, *114*, 735–751, doi:10.1086/507617.
- Wang, T., B. M. Jahn, V. P. Kovach, Y. Tong, D. W. Hong, and B. F. Han (2009), Nd-Sr isotopic mapping of the Chinese Altai and implications for continental growth in the Central Asian Orogenic Belt, *Lithos*, *110*(1–4), 359–372, doi:10.1016/j.lithos.2009.02.001.
- Wang, Y., W. D. Mooney, X. Yuan, and R. G. Coleman (2003), The crustal structure from the Altai Mountains to the Altyn Tagh Fault, northwest China, *J. Geophys. Res.*, *108*(B6), 2322, doi:10.1029/2001JB000552.

- Wang, Y., C. Yuan, X. Long, M. Sun, W. Xiao, G. Zhao, K. Cai, and Y. Jiang (2011), Geochemistry, zircon U–Pb ages and Hf isotopes of the Paleozoic volcanic rocks in the northwestern Chinese Altai: Petrogenesis and tectonic implications, *J. Asian Earth Sci.*, *42*(5), 969–985, doi:10.1016/j.jseas.2010.11.005.
- Wei, C., G. Clarke, W. Tian, and L. Qiu (2007), Transition of metamorphic series from the Kyanite- to andalusite-types in the Altai orogen, Xinjiang, China: Evidence from petrography and calculated KFMASH and KFMASH phase relations, *Lithos*, *96*(3–4), 353–374, doi:10.1016/j.lithos.2006.11.004.
- Wellman, P. (1988), Development of the Australian Proterozoic crust as inferred from gravity and magnetic anomalies, *Precambrian Res.*, *40–41*, 89–100, doi:10.1016/0301-9268(88)90062-9.
- White, R. W., R. Powell, and T. J. B. Holland (2007), Progress relating to calculation of partial melting equilibria for metapelites, *J. Metamorph. Geol.*, *25*(5), 511–527, doi:10.1111/j.1525-1314.2007.00711.x.
- Wilhelm, C., B. F. Windley, and G. M. Stampfli (2012), The Altaids of Central Asia: A tectonic and evolutionary innovative review, *Earth Sci. Rev.*, *113*(3–4), 303–341, doi:10.1016/j.earscirev.2012.04.001.
- Windley, B. F., A. Kröner, J. Guo, Q. Gu, Y. Li, and C. Zhang (2002), Neoproterozoic to Paleozoic geology of the Altai Orogen, NW China: New zircon age data and tectonic evolution, *J. Geol.*, *110*(6), 719–737, doi:10.1086/342866.
- Windley, B. F., D. Alexeiev, W. J. Xiao, A. Kröner, and G. Badarch (2007), Tectonic models for accretion of the Central Asian Orogenic Belt, *J. Geol. Soc. London*, *164*, 31–47, doi:10.1144/0016-76492006-022.
- Wolf, M. B., and P. J. Wyllie (1994), Dehydration-melting of amphibolite at 10kbar: The effects of temperature and time, *Contrib. Mineral. Petrol.*, *115*(4), 369–383, doi:10.1007/bf00320972.
- Wong, K., M. Sun, G. Zhao, C. Yuan, and W. Xiao (2010), Geochemical and geochronological studies of the Alegendayi Ophiolitic Complex and its implication for the evolution of the Chinese Altai, *Gondwana Res.*, *18*, 438–454, doi:10.1016/j.gr.2010.01.010.
- Xiao, W. J., et al. (2009), Paleozoic multiple subduction-accretion processes of the southern Altaids, *Am. J. Sci.*, *309*(3), 221–270, doi:10.2475/03.2009.02.
- Xu, J. F., P. R. Castillo, F. R. Chen, H. C. Niu, X. Y. Yu, and Z. P. Zhen (2003), Geochemistry of late Paleozoic mafic igneous rocks from the Kuerti area, Xinjiang, northwest China: Implications for backarc mantle evolution, *Chem. Geol.*, *193*(1–2), 137–154, doi:10.1016/S0009-2541(02)00265-6.
- Yakymchuk, C., C. S. Siddoway, C. M. Fanning, R. McFadden, F. J. Korhonen, and M. Brown (2013), Anatexitic reworking and differentiation of continental crust along the active margin of Gondwana: A zircon Hf–O perspective from West Antarctica, in *Antarctica and Supercontinent Evolution*, vol. 383, edited by S. L. Harley, I. C. W. Fitzsimons, and Y. Zhao, pp. 169–210, Geol. Soc. London Spec. Publ., doi:10.1144/sp383.7.
- Yang, F., J. W. Mao, S. Yan, F. Liu, F. Chai, G. Zhou, G. Liu, L. He, X. Geng, and J. Dai (2008), Geochronology, geochemistry and geological implications of the Mengku synorogenic plagiogranite pluton in Altai, Xinjiang [in Chinese with English abstract], *Acta Geol. Sin.*, *82*(4), 485–499.
- Yuan, C., M. Sun, W. Xiao, X. Li, H. Chen, S. Lin, X. Xia, and X. Long (2007), Accretionary orogenesis of the Chinese Altai: Insights from Paleozoic granitoids, *Chem. Geol.*, *242*, 22–39, doi:10.1016/j.chemgeo.2007.02.013.
- Zhang, C., C. Wei, and R. Hou (2007), Phase equilibrium of low-pressure metamorphism in the Altai, Xinjiang [in Chinese with English abstract], *Geol. China*, *34*(1), 34–41.
- Zhang, H., H. Niu, X. Yu, H. Sato, J. I. Ito, and Q. Shan (2003), Geochemical characteristics of the Shaerbulake boninites and their tectonic significance, Fuyun County, northern Xinjiang [in Chinese with English abstract], *China, Geochemica*, *32*(2), 155–160.
- Zhang, J., M. Sun, K. Schulmann, G. Zhao, Q. Wu, Y. Jiang, A. Guy, and Y. Wang (2015), Distinct deformational history of two contrasting tectonic domains in the Chinese Altai: Their significance in understanding accretionary orogenic process, *J. Struct. Geol.*, *73*, 64–82, doi:10.1016/j.jsg.2015.02.007.
- Zhao, J., G. Liu, Z. Lu, X. Zhang, and G. Zhao (2003), Lithospheric structure and dynamic processes of the Tianshan orogenic belt and the Junggar basin, *Tectonophysics*, *376*(3–4), 199–239, doi:10.1016/j.tecto.2003.07.001.
- Zhao, Z., Q. Wang, X. Xiong, H. C. Niu, H. Zhang, and Y. Qiao (2007), Magnesian igneous rocks in northern Xinjiang [in Chinese with English abstract], *Acta Geol. Sin.*, *23*(7), 1696–1707.
- Zhuang, Y. (1994), The pressure-temperature-space-time (P–T–S–t) evolution of metamorphism and development mechanism of the thermal-structural-gneiss domes in the Chinese Altaides [in Chinese with English abstract], *Acta Geol. Sin.*, *68*(1), 35–47.
- Ziegler, P. A. (1986), Geodynamic model for the Palaeozoic crustal consolidation of Western and Central Europe, *Tectonophysics*, *126*(2), 303–328, doi:10.1016/0040-1951(86)90236-2.
- Zorigtkhuu, O. E., T. Tsunogae, and B. Dash (2011), Metamorphic P–T evolution of garnet–kyanite–staurolite schist and garnet amphibolite from Bodonch area, western Mongolian Altai: Geothermobarometry and mineral equilibrium modeling, *J. Asian Earth Sci.*, *42*(3), 306–315, doi:10.1016/j.jseas.2011.04.026.
- Zou, T. R., H. Z. Cao, and B. Q. Wu (1988), Orogenic or anorogenic granitoids of the Altai Mountains, Xinjiang and their discrimination criteria [in Chinese with English abstract], *Acta Geol. Sin.*, *62*, 228–245.